



**NAVAL  
POSTGRADUATE  
SCHOOL**

**MONTEREY, CALIFORNIA**

**THESIS**

**EFFECTS OF HYDROPHOBIC COATINGS  
ON POLYBENZOXAZOLE FIBERS  
UNDER BALLISTIC LOADING**

by

Beatrice Joyce A. Cayaban

December 2020

Thesis Advisor:  
Second Reader:

Raymond M. Gamache  
Abram H. Clark IV

**Approved for public release. Distribution is unlimited.**

**THIS PAGE INTENTIONALLY LEFT BLANK**

<b>REPORT DOCUMENTATION PAGE</b>			<i>Form Approved OMB No. 0704-0188</i>	
Public reporting burden for this collection of information is estimated to average 1 hour per response, including the time for reviewing instruction, searching existing data sources, gathering and maintaining the data needed, and completing and reviewing the collection of information. Send comments regarding this burden estimate or any other aspect of this collection of information, including suggestions for reducing this burden, to Washington headquarters Services, Directorate for Information Operations and Reports, 1215 Jefferson Davis Highway, Suite 1204, Arlington, VA 22202-4302, and to the Office of Management and Budget, Paperwork Reduction Project (0704-0188) Washington, DC, 20503.				
<b>1. AGENCY USE ONLY (Leave blank)</b>		<b>2. REPORT DATE</b> December 2020	<b>3. REPORT TYPE AND DATES COVERED</b> Master's thesis	
<b>4. TITLE AND SUBTITLE</b> EFFECTS OF HYDROPHOBIC COATINGS ON POLYBENZOXAZOLE FIBERS UNDER BALLISTIC LOADING			<b>5. FUNDING NUMBERS</b>	
<b>6. AUTHOR(S)</b> Beatrice Joyce A. Cayaban				
<b>7. PERFORMING ORGANIZATION NAME(S) AND ADDRESS(ES)</b> Naval Postgraduate School Monterey, CA 93943-5000			<b>8. PERFORMING ORGANIZATION REPORT NUMBER</b>	
<b>9. SPONSORING / MONITORING AGENCY NAME(S) AND ADDRESS(ES)</b> N/A			<b>10. SPONSORING / MONITORING AGENCY REPORT NUMBER</b>	
<b>11. SUPPLEMENTARY NOTES</b> The views expressed in this thesis are those of the author and do not reflect the official policy or position of the Department of Defense or the U.S. Government.				
<b>12a. DISTRIBUTION / AVAILABILITY STATEMENT</b> Approved for public release. Distribution is unlimited.			<b>12b. DISTRIBUTION CODE</b> A	
<b>13. ABSTRACT (maximum 200 words)</b> <p>Polybenzoxazole fibers (PBO, commercially trademarked as Zylon) were once used as an alternative to ultra-high molecular weight polyethylene (UHMWPE) fibers in body armor systems. PBO fibers exhibit a high Young's modulus, excellent thermal stability, and tensile strength (nearly twice that of Kevlar), but the physical properties severely degrade when exposed to water. Hydrophobic polymer coatings were applied to PBO fibers and studied for moisture resistance, coating durability, and ballistic performance. Instron tensile testing and a V50 assessment utilizing a light gas gun and 9.525 mm spherical chromium-steel projectiles were conducted on four different textile armor systems, including uncoated PBO weave, uncoated PBO weave exposed to water, polymer-coated PBO weave, and polymer-coated PBO weave exposed to water. Using load cells to measure uni-axial forces, combined with digital image correlation enabling measurement of both in-plane and out-of-plane fiber deflection, stress-strain measurements of the four different textile armor systems were measured and compared. Flex Seal liquid coating proved to be the most effective waterproof coating in terms of consistent hydrophobic performance, flexibility, and ease of application; however, further research is required to refine coating methods as well as collect additional data for the performance of PBO under dynamic loads.</p>				
<b>14. SUBJECT TERMS</b> composite materials, stress strain relations, molecular weight, ballistics, fibers, polyethylenes, body armor, thesis, test and evaluation, polybenzoxazole			<b>15. NUMBER OF PAGES</b> 79	
			<b>16. PRICE CODE</b>	
<b>17. SECURITY CLASSIFICATION OF REPORT</b> Unclassified	<b>18. SECURITY CLASSIFICATION OF THIS PAGE</b> Unclassified	<b>19. SECURITY CLASSIFICATION OF ABSTRACT</b> Unclassified	<b>20. LIMITATION OF ABSTRACT</b> UU	

THIS PAGE INTENTIONALLY LEFT BLANK

**Approved for public release. Distribution is unlimited.**

**EFFECTS OF HYDROPHOBIC COATINGS ON POLYBENZOXAZOLE  
FIBERS UNDER BALLISTIC LOADING**

Beatrice Joyce A. Cayaban  
Lieutenant, United States Navy  
BS, U.S. Naval Academy, 2014

Submitted in partial fulfillment of the  
requirements for the degree of

**MASTER OF SCIENCE IN APPLIED PHYSICS**

from the

**NAVAL POSTGRADUATE SCHOOL  
December 2020**

Approved by: Raymond M. Gamache  
Advisor

Abram H. Clark IV  
Second Reader

Kevin B. Smith  
Chair, Department of Physics

THIS PAGE INTENTIONALLY LEFT BLANK

## **ABSTRACT**

Polybenzoxazole fibers (PBO, commercially trademarked as Zylon) were once used as an alternative to ultra-high molecular weight polyethylene (UHMWPE) fibers in body armor systems. PBO fibers exhibit a high Young's modulus, excellent thermal stability, and tensile strength (nearly twice that of Kevlar), but the physical properties severely degrade when exposed to water. Hydrophobic polymer coatings were applied to PBO fibers and studied for moisture resistance, coating durability, and ballistic performance. Instron tensile testing and a V50 assessment utilizing a light gas gun and 9.525 mm spherical chromium-steel projectiles were conducted on four different textile armor systems, including uncoated PBO weave, uncoated PBO weave exposed to water, polymer-coated PBO weave, and polymer-coated PBO weave exposed to water. Using load cells to measure uni-axial forces, combined with digital image correlation enabling measurement of both in-plane and out-of-plane fiber deflection, stress-strain measurements of the four different textile armor systems were measured and compared. Flex Seal liquid coating proved to be the most effective waterproof coating in terms of consistent hydrophobic performance, flexibility, and ease of application; however, further research is required to refine coating methods as well as collect additional data for the performance of PBO under dynamic loads.

THIS PAGE INTENTIONALLY LEFT BLANK

# TABLE OF CONTENTS

<b>I.</b>	<b>INTRODUCTION.....</b>	<b>1</b>
<b>II.</b>	<b>BACKGROUND .....</b>	<b>3</b>
	<b>A. OVERVIEW OF BALLISTIC FIBERS .....</b>	<b>3</b>
	<b>B. OVERVIEW OF HYDROPHOBIC COATINGS .....</b>	<b>10</b>
<b>III.</b>	<b>EXPERIMENTAL SETUP .....</b>	<b>13</b>
	<b>A. PROCESS OVERVIEW .....</b>	<b>13</b>
	<b>B. HYDROPHOBIC COATING TRIALS.....</b>	<b>14</b>
	<b>C. ZYLON TENSILE TESTING .....</b>	<b>18</b>
	<b>D. V<sub>50</sub> ASSESSMENT.....</b>	<b>22</b>
<b>IV.</b>	<b>DATA .....</b>	<b>31</b>
	<b>A. HYDROPHOBIC COATINGS RESULTS .....</b>	<b>31</b>
	<b>1. COMMERCIAL OFF-THE-SHELF COATINGS.....</b>	<b>31</b>
	<b>2. INDUSTRIAL-GRADE COATINGS .....</b>	<b>32</b>
	<b>3. LEADING COATING TESTS .....</b>	<b>33</b>
	<b>B. INSTRON TENSILE TEST RESULTS.....</b>	<b>33</b>
	<b>C. V<sub>50</sub> RESULTS.....</b>	<b>40</b>
<b>V.</b>	<b>DATA ANALYSIS .....</b>	<b>45</b>
	<b>A. HYDROPHOBIC COATINGS ANALYSIS .....</b>	<b>45</b>
	<b>B. INSTRON TENSILE TEST ANALYSIS .....</b>	<b>47</b>
	<b>C. V<sub>50</sub> ASSESSMENT ANALYSIS .....</b>	<b>48</b>
<b>VI.</b>	<b>CONCLUSION .....</b>	<b>53</b>
	<b>A. OVERVIEW.....</b>	<b>53</b>
	<b>B. CHALLENGES.....</b>	<b>54</b>
	<b>C. FUTURE RESEARCH.....</b>	<b>55</b>
	<b>APPENDIX A .....</b>	<b>57</b>
	<b>LIST OF REFERENCES.....</b>	<b>61</b>
	<b>INITIAL DISTRIBUTION LIST .....</b>	<b>63</b>

THIS PAGE INTENTIONALLY LEFT BLANK

## LIST OF FIGURES

Figure 1.	Graphical representation of the genealogy of super fibers. Red stars represent important discoveries or advancements in the field. White circles represent when a fiber was commercialized. Source: [2].	3
Figure 2.	Hydrogen bonding in Kevlar fibers. Source: [6].	4
Figure 3.	Historical change of tensile strength in ballistic fibers. Source: [2].	5
Figure 4.	Hosemann's structure model of the stretched linear polyethylene. Source: [2].	6
Figure 5.	Modeled representation of UHMWPE composites for flexible (a) and stiff (b) applications. Source: [7].	7
Figure 6.	Chemical reaction for polybenzoxazole (PBO). Source: [6].	9
Figure 7.	Water contact indicator placement on coating samples.	15
Figure 8.	Activated water contact indicator stickers. Note the spreading of the red dye from the stickers due to moisture exposure.	15
Figure 9.	Placement of tape around edges of coating sample.	16
Figure 10.	Fog chamber apparatus.	17
Figure 11.	Zylon sample on a scanning electron microscope slide.	19
Figure 12.	Taking strand measurements utilizing the scanning electron microscope.	20
Figure 13.	Zylon samples prepped for tensile testing.	21
Figure 14.	Instron tensile testing machine with attached load cell for elongation measurements.	21
Figure 15.	Breech, barrel, and catch tank of the light gas gun.	22
Figure 16.	Valve and firing control system for the light gas gun.	23
Figure 17.	Chromium steel sphere and four-piece serrated sabot.	24
Figure 18.	Frame with uncoated, unexposed Zylon weft sample, post-shot.	25
Figure 19.	Data collection system for the light gas gun.	26

Figure 20.	Placement of the break sheet on the center of the sample wefts.....	27
Figure 21.	Placement of the break sheet on the stripper plate.....	28
Figure 22.	Placement of backing tape behind the sample wefts. ....	29
Figure 23.	Camera and lighting setup for experiment image capture. ....	29
Figure 24.	Clear polycarbonate plates attached to catch tank. ....	30
Figure 25.	SEM width measurements of unexposed PBO fiber strands. ....	34
Figure 26.	SEM width measurements of PBO fiber strands exposed to heat (50°C) and moisture for 96 hours. ....	35
Figure 27.	SEM slide with individual PBO fiber strands.....	36
Figure 28.	PBO fiber weft being separated from a Zylon woven sheet. ....	36
Figure 29.	Mettler Toledo AB104-S analytical balance, used for measuring mass of PBO wefts.....	37
Figure 30.	Stress-strain curve for uncoated unexposed PBO.....	38
Figure 31.	Stress-strain curve for uncoated exposed PBO.....	39
Figure 32.	Stress-strain curve for coated exposed PBO.....	39
Figure 33.	Vertical load cell data comparisons V50 partial penetration samples. ....	42
Figure 34.	Horizontal load cell data comparisons V50 partial penetration samples.....	42
Figure 35.	Vertical load cell data comparisons V50 complete penetration samples.....	43
Figure 36.	Horizontal load cell data comparisons V50 complete penetration samples.....	43
Figure 37.	Moment of peak deflection for uncoated unexposed PBO. ....	49
Figure 38.	Moment of peak force on second layer of uncoated unexposed PBO. The projectile has already exited the sample. ....	49

## LIST OF TABLES

Table 1.	List of tested commercial and industrial grade hydrophobic coatings. ....	14
Table 2.	Waterproof coating sample sets. ....	17
Table 3.	Zylon tensile test sample sets. ....	18
Table 4.	V <sub>50</sub> assessment sample sets. ....	25
Table 5.	Commercial off-the-shelf coating data sets. ....	31
Table 6.	Industrial-grade coating data sets. ....	32
Table 7.	Leading coating data set. ....	33
Table 8.	Initial PBO sample SEM and Instron data. PBO was exposed to heat and water for 96 hours. ....	34
Table 9.	Instron tensile test results. ....	38
Table 10.	Additional coating tensile test results. ....	40
Table 11.	V <sub>50</sub> penetration velocities for each PBO sample set. ....	41

THIS PAGE INTENTIONALLY LEFT BLANK

## LIST OF ACRONYMS AND ABBREVIATIONS

COTS	commercial off the shelf
Dyneema	commercial UHMWPE fiber manufactured by DSM
LabVIEW	Laboratory Virtual Instrument Engineering Workbench
LVDT	linear variable differential transformer
PBO	polybenzoxazole
SEM	scanning electron microscope
Technora	commercial para-aramid manufactured by Teijin
UHMWPE	ultra-high molecular weight polyethylene
Zylon	commercial PBO manufactured by Toyobo

THIS PAGE INTENTIONALLY LEFT BLANK

## I. INTRODUCTION

Modern armor seeks to increase mass efficiency performance through either blunting the incident projectile or increasing the time given to arrest the projectile. Both techniques decrease the dynamic pressure on the armor system. Many new advanced armor systems, however, incorporate both. Current blunting techniques incorporate ceramics with a high enough material hardness to blunt the incident projectiles, decreasing the impact pressure. Textiles enable an increase in the time it takes to arrest the projectile, additionally reducing the impact pressure on the armor system. Key objectives to increase armor performance include the development of high-strength low-density ceramics and high tensile strength textiles. This thesis focuses on the latter, where high-strength textile fibers will be investigated as improvements to the current textile systems used within body armor systems.

Polybenzoxazole (otherwise known as PBO and commercially trademarked as Zylon) fibers were once used as an alternative to Kevlar and other similar para-aramid fibers incorporated within body armor systems. PBO fibers exhibit a high Young's modulus, excellent thermal stability, a strain wave velocity of over 800 m/s, and a tensile strength nearly twice that of Kevlar [1].

PBO was experimented with since the 1980s but commercialized by Toyobo Co., Ltd., one of Japan's top textile manufacturers, in 1998. PBO became popular for use in recreational sports equipment, medical instruments, space systems, and other functions where thermal stability and high strength were key [2]. Its high tensile strength compared to other competitive super fibers like Technora para-aramids and ultra-high molecular weight polyethylenes such as Dyneema made it an attractive choice as a stronger ballistic fiber similar in weight and flexibility to Kevlar.

In 2003, two law enforcement officers suffered injuries while wearing Zylon body armor, leading to the death of one and severe injury to the other. Investigations led by the National Institute of Justice concluded that repeated exposure to moisture had decreased the strength of the PBO in the armor by 30%, providing insufficient protection against

common high-velocity projectiles. By 2006, all body armor containing PBO was pulled off the market, though a multitude of lawsuits that stemmed from the original incidents continue to this day [3].

While there may be ways to improve PBO during its manufacturing process, the simplest method to avoid hygroscopic physical performance degradation is to apply a hydrophobic coating on to ready-made PBO fiber. To preserve the beneficial properties of PBO the coating must also be lightweight, abrasion resistant, and flexible, while not altering the chemical composition of the PBO itself. Many commercial and industrial polymers, including polyureas, satisfy these requirements, such as styrenic block copolymers from Kraton Corporation and Swift Response, LLC's Flex Seal. While several companies were rumored to have begun studies in hydrophobic coatings for PBO, ongoing lawsuits and the existing controversy surrounding Zylon have discouraged making any results public knowledge.

This research seeks to reintroduce PBO fiber into body armor applications through the development of a hydrophobic coating system which helps prevent performance degradation when exposed to high-moisture environments. Within this study, several commercial and industrial polymer coatings will be tested for thickness, flexibility, and water resistance when applied to PBO fiber. Performance of PBO armor will be assessed using multiple techniques, including tensile testing and ballistic impact studies (light gas gun), to determine variations in performance based on diverse exposure and coating systems for Zylon.

## II. BACKGROUND

### A. OVERVIEW OF BALLISTIC FIBERS

Though personal body armor has been an interest in civilization since the invention of weapons, it was not until the past century that advances in textile armor truly made a debut. This is mainly attributed to the gradual change in threat profile, from blunt or slashing weapons that could be stopped by leather or metal, to the high-velocity projectiles of today's modern age. While layers of silk were found to be effective at stopping the slow-moving bullets of revolvers in the late 1800s [4], as gun technology advanced so did the demand for better protective armor.

Beginning with the appearance of Nylon and Rayon during World War 2 (Figure 1), a string of major discoveries in the realm of super fibers sprang forth in the 20th and 21st centuries. The engineering focus shifted towards fiber polymers that could be used in lightweight armor systems. Reinforced by Doron armor plates, a laminate made of fiberglass, and later hard ceramic plates, Nylon became a principal inclusion in body armor throughout the Korean War [5].

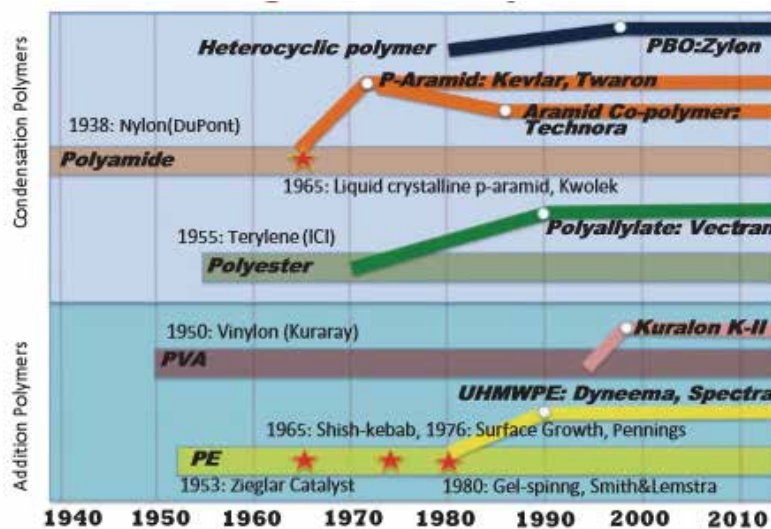


Figure 1. Graphical representation of the genealogy of super fibers. Red stars represent important discoveries or advancements in the field. White circles represent when a fiber was commercialized. Source: [2].

In the mid-1960s, Stephanie Kwolek of the DuPont Company discovered para-aramid polymers in a liquid crystalline state. While a meta-type, heat-resistant aramid fiber had already been marketed by DuPont, it was Kwolek's findings that demonstrated a para-aramid solution capable of self-organizing into a nematic liquid crystalline state. From this, Kevlar was born, a synthetic fiber having five times the tensile strength of steel when woven and layered [2].

At the time called poly-para-phenylene terephthalamide (PPTA), Kevlar began as a fiber with very low tensile strength until the development of air-gap wet spinning in 1970. Para-aramid (specifically Kevlar) molecules have a characteristic rigidity due to the carbon-nitrogen partial double bond of the amide group [6]. While the rigid molecules in para-aramids were prone to orienting themselves parallel to each other in order to give the fiber its characteristic tensile strength, this orientation only spanned micrometers in regions known as "domains."

Domains often differed from each other to the effect that the orientation of the para-aramid solution overall could be considered random in its static state. Gel spinning allowed for a shear or extensional flow to be applied to an output of the solution, orienting the molecules parallel to the para-aramid fiber while being held together in the transverse direction by hydrogen bonds, increasing its tensile strength, as seen in Figure 2 [2].

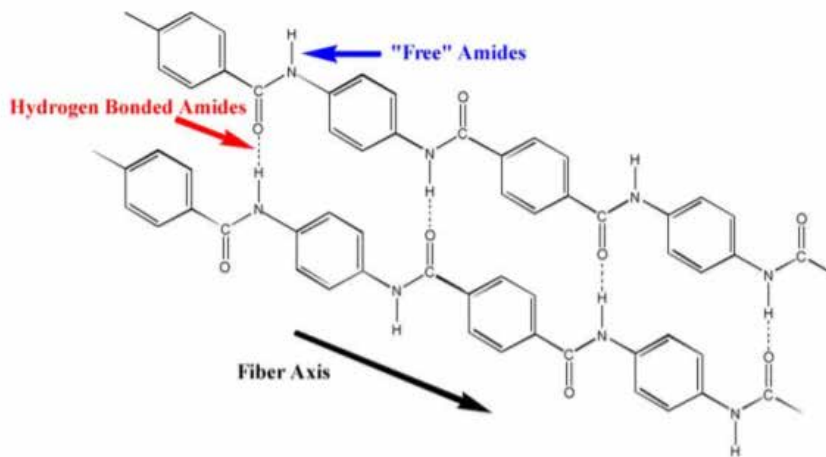


Figure 2. Hydrogen bonding in Kevlar fibers. Source: [6].

This led directly to the commercialization of Kevlar as a high-strength fiber, to be used in the mid-1970s as body armor following a National Institute of Justice program looking to create lightweight armor for U.S. law enforcement. By 1976, companies began marketing vests made solely of Kevlar [2].

Other companies began to build on the success of Kevlar in the body armor market, most notably the improved aramid Technora by Teijin Aramid, as well as the UHMWPE Dyneema by DSM. Historical tensile strengths for both can be found in Figure 3. Technora aramids, first manufactured in 1987, boasted a tensile strength of nearly 3.4 GPa (compared to Kevlar’s 3.0 GPa), with a high chemical and heat resistance, as well as resistance to UV light, which is known to degrade Kevlar. Kevlar also has a propensity for absorbing moisture with a 3.5% moisture regain compared to Technora’s 2.0% [2], disrupting the hydrogen bonds between the rigid para-aramid molecules in the transverse direction. Dyneema and other brands of UHMWPE outstrip these aramids even further, with a tensile strength of 3.6 GPa, along with improved resistance to chemicals, UV light, and moisture [7].

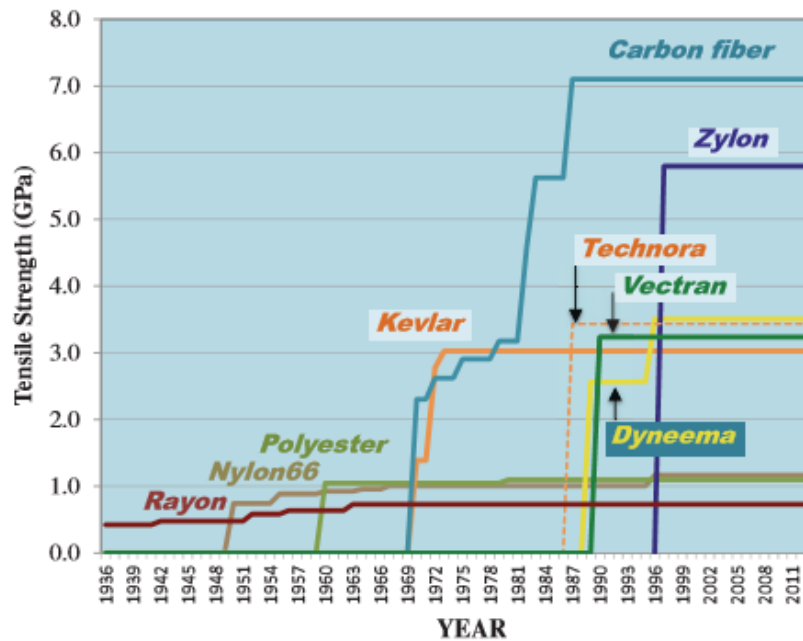


Figure 3. Historical change of tensile strength in ballistic fibers. Source: [2].

UHMWPE advancement is based on a “shish-kebab” structure, found in stirred solutions of UHMWPE in 1963–1965. Crystalline polymers are known to form into a rounded structure called “spherulite,” where molecular alignment radiates outward from a center and the folded chain structure is mostly perpendicular to it, intertwining to form amorphous regions between these radial alignments. A shish-kebab structure, however, consists of two parts: a centerline of extended chain crystals, and branches of folded chain crystals. Where para-aramids relied on hydrogen bonds and Van der Waals forces of parallel alignments to connect molecules, UHMWPE’s shish-kebab structure allowed for tighter bonds as the branches of the folded chain crystals interlaced, leading to higher tensile strength [2].

Originally theorized to have a tensile strength of 25–31 GPa, commercially UHMWPE has only managed to achieve a tensile strength of 3–4 GPa. This can be attributed to the fundamental molecular structure of polyethylenes, which can range from the order of nanometers to millimeters and contains multiple types of microdefects in the macrolattice, as seen in Figure 4.

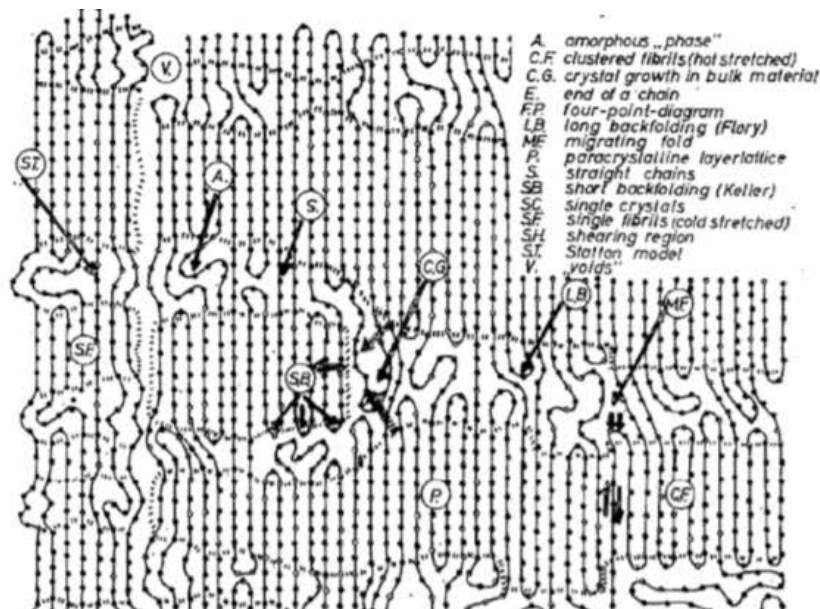


Figure 4. Hosemann’s structure model of the stretched linear polyethylene.  
Source: [2].

Polyethylene fibers tend to be riddled with free-floating molecular branches that are prone to entanglement, resulting in a lower tensile strength. An ideal UHMWPE structure would have densely packed and parallel molecules along the fiber's axis, with as few defects as possible. Like Kevlar before it, UHMWPE also benefitted from the development of a gel spinning process specifically for Dyneema, which helped to force a parallel orientation despite the continuation of defects and inconsistencies in its molecular structure [2].

UHMWPE must also be stitched and covered with a thin polymer film (for flexible applications) or heat-pressed (for stiff applications) into unidirectional layers, arranged in alternating  $0^{\circ}/90^{\circ}$  composite sheets pictured in Figure 5. This is due to the lower performance in woven UHMWPE caused by the low frictional coefficient of UHMWPE [7].

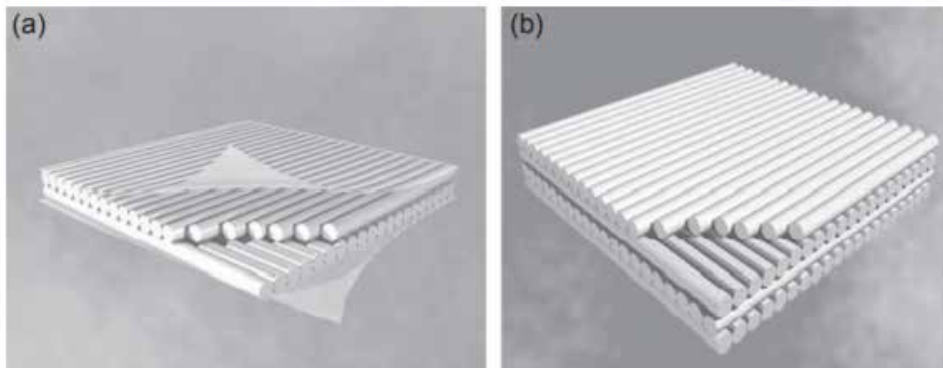


Figure 5. Modeled representation of UHMWPE composites for flexible (a) and stiff (b) applications. Source: [7].

Of the two UHMWPE composites the stiff heat-pressed plates are stronger, and the loss of flexibility and low melting point became major limitations in ballistic armor applications. Despite this, Dyneema maintains several advantages to para-aramid fibers, including 0% moisture regain, abrasion resistance, easy fabrication, and a high tensile strength surpassed only by PBO [2]. Currently, high performance body armor is made of ceramic plates backed by pressed UHMWPE. The hard ceramic effectively blunts the projectile, while the UHMWPE is used to catch and arrest projectiles after impacting the front ceramic plate.

This phenomenon can be explained using the Cunniff and Auerbach equation for the assessment of ballistic fibers. Utilizing dimensional analysis, Cunniff and Auerbach discovered that the most direct way to relate the  $V_{50}$  performance of armor systems (the velocity at which the probability of penetration is 50%) to a projectile is with the product of elastic energy storage capability of the fiber per unit mass and strain wave velocity, otherwise known as the  $(U^*)^{1/3}$  parameter. Ballistic fiber performance can then be measured using only fundamental mechanical properties in the equation

$$\left[ U^* \left\{ \frac{m^3}{s^3} \right\} \right]^{1/3} = \left[ \frac{\sigma \varepsilon}{2\rho} \sqrt{\frac{E}{\rho}} \right]^{1/3} \quad (1)$$

where  $\sigma$  is the ultimate axial tensile strength of the fiber,  $\varepsilon$  is the ultimate tensile strain of the fiber,  $\rho$  is the fiber density, and  $E$  is the linear elastic modulus of the fiber. This is further simplified when fibers can be considered linearly elastic wherein  $\sigma = E\varepsilon$ , and the equation relies solely on the fiber's tensile strength, density, and strain-to-failure, which can all be measured through experiment. Of all currently available ballistic fibers, the  $(U^*)^{1/3}$  parameter for polybenzoxazole ranks the highest [6].

In 1998, the PBO Zylon was developed by Toyobo. Polybenzazole (PBZ) chemistry had been experimented with since the late 1960s, after the technique for creating high molecular weight PBZ by using polyphosphoric acid (PPA) as a solvent and dehydrating agent was developed [2]. PBO is prepared when 1,3-diamino-4,6-dihydroxybenzene (DADHB) reacts with terephthalic acid (TA) or PPA, forming a polymer molecular structure with a characteristic benzoxazole ring, as seen in Figure 6. Though both Kevlar and Zylon contain parallel-orienting, repeating units connected by hydrogen bonds that stack in their liquid crystalline state, Zylon has a larger molecule that forms a more rigid structure, increasing the strength of chain interactions and resulting in the chains better orienting in one direction [6].

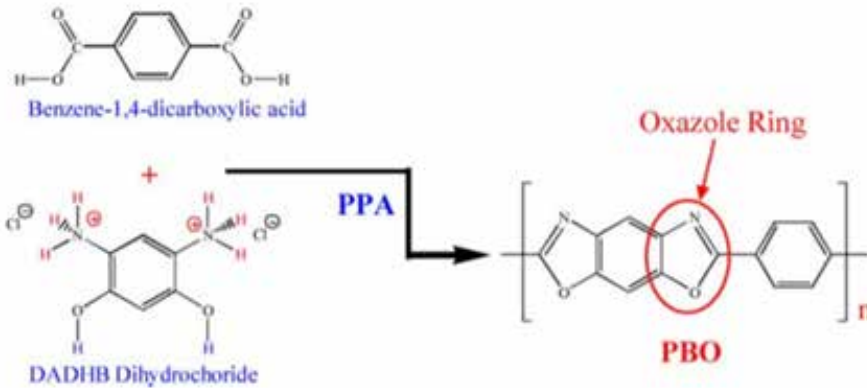


Figure 6. Chemical reaction for polybenzoxazole (PBO). Source: [6].

With a tensile strength of almost 5.8 GPa and a 3.5% elongation at break [1], Zylon is nearly twice as strong as Kevlar, and more than 2.0 GPa stronger than any UHMWPE on the market [2]. In addition, where UHMWPE must be heat-pressed or layered for use in ballistic armor (becoming non-compliant), Zylon is able to retain its effectiveness against projectiles as a flexible single-layer weave. This made it an attractive alternative to Dyneema for many applications, including body armor.

The first possible noted indication towards performance loss in PBO exposed to moisture-rich conditions was in 1930, when research showed the benzoxazole ring appeared more unstable in wet environments. During benzoxazole hydrolysis, 2-hydroxy-benzoxazoline is formed; an intermediate molecule usually found in imidazoles and thiazoles, 2-hydroxy-benzoxazoline collapses into degradation products like those from C-N and C-O fission [6]. This hydrolytic degradation, however, is not enough to completely break down most amides [2]. Prolonged exposure to heat is also required—but as the oxazole ring found in PBO has a lower aromatic stability than imidazoles and thiazoles, it is possible that it has a lower temperature threshold for degradation as well. This raised concerns about using PBO in personal protective equipment, as one weak link in PBO's rigid chain caused by hydrolytic degradation affected the strength of the entire structure [6].

Since the incidents regarding the use of Zylon in body armor from 2003 and its subsequent removal from the commercial market, several advancements have been made

in PBO fabrication. Most relevant to this research is the Toyobo's creation of Zylon HM, which stands for "high modulus," and what will be used in all experiments. It has earned its name by its large tensile modulus (170 cN/dtex), but also has an improved 0.6% moisture regain compared to the as-spun Zylon's 2.0% [1].

## **B. OVERVIEW OF HYDROPHOBIC COATINGS**

The creation of a hydrophobic coating is not a new concept, which is what makes it difficult to choose one best suited for waterproofing PBO. Hydrophobic materials are made of molecules with hydrocarbon chains or other nonpolar region, that are unable to form hydrogen bonds. The hydrogen bonds are then disrupted and oriented tangential to the nonpolar region, effectively "repelling" water molecules. Most hydrophobic coatings rely on this mechanism of tightly structured nonpolar materials with relatively high surface energy to repel water. Hydrophobic materials usually have at least a 90° contact angle with water.

Thermoset or thermoplastic materials are often associated with hydrophobic coatings for ballistic applications; thermoset materials (polyester, epoxy, phenolic, vinyl ester) can be used to turn ballistic fibers into rigid structures known for their strength and thermal properties, while thermoplastics (polyethylene, acrylic polymer, polyamide, polyurethane) help increase ballistic fracture toughness [8].

Within the investigation for hydrophobic coatings, the coatings chosen for testing were selected based on the criteria of being commercial off the shelf (COTS). To preserve the mass efficiency of PBO fiber, coatings had to be relatively lightweight, thin, and flexible, in addition to having excellent hydrophobic and UV resistant properties. In addition, the coatings must be transparent or translucent to enable visible inspection of moisture indicators which change colors when exposed to moisture.

For commercial products, although polyurethanes and polyureas were the initial focus, coating materials trended towards waterproofing sealants. Of these, the most promising was Flex Seal; manufactured by Swift Response, Flex Seal is an elastomer copolymer that cures when exposed to moisture in the air. Other coatings tested were standard thermoplastic, HERCO fishpond coating, Creature Cast Rubber flexible costume-

grade neoprene, and rubberized coatings like Performix Plasti Dip and Rust-oleum Leak Seal. These coatings often ran thin, flexible, and in pre-mixed cans or spray canisters, making them attractive options when it considering ease-of-use.

For industrial-grade products, coatings were chosen exclusively from the synthetic rubber manufacturing company, Kraton Corporation. Founded in the 1950s as part of the Shell Chemical Company during the United States' push for synthetic rubbers, Kraton specializes in styrenic block copolymers for adhesives, packaging, coating, and moldable material creation. Most of their polymers have a two-glass transition temperature (a rubber around  $-40^{\circ}\text{C}$  and a polystyrene around  $110^{\circ}\text{C}$ ) and hold up well to UV exposure, though prolonged exposure will require stabilizers. All the polymers dissolve in nonpolar solvents like toluene and xylene at room temperature [9].

Technical consultation with Kraton revealed five coatings chosen for their elongation and thermal properties, as well as ease of coating application. Three of the five coatings are market development grade, used as polymer modifiers and the formulation of adhesives and coatings (MD6951, MD1648, and MD1653). One is an FG series SEBS polymer with maleic anhydride grafting (FG1924) to improve its adhesion to substrates, making it a popular choice for the creation of engineering thermoplastic materials. The last is G series SEBS polymer (G1657), which has the highest strength of the Kraton styrene thermoplastic block copolymers [10].

THIS PAGE INTENTIONALLY LEFT BLANK

### **III. EXPERIMENTAL SETUP**

#### **A. PROCESS OVERVIEW**

This thesis seeks to demonstrate the preserved ballistic performance of PBO when encapsulated within a hydrophobic coating. Studies within this thesis will expose the encapsulated PBO to moisture for a long period of time (96 hours), followed by a physical assessment of near-static and dynamic tensile strength. The investigation was performed in three key parts: hydrophobic coating studies, Instron tensile testing, and a light gas gun ballistic  $V_{50}$  assessment.

Within the hydrophobic coating studies, several commercially and industrially available coatings claiming to be either water resistant or waterproof were applied to nominally five layers of 20 cm by 20 cm cotton fabric sheets with water exposure indicators that change colors (white to red) when exposed to water. These coated fabric sheets were continuously exposed to both water spray and water submersion for a period of up to 96 hours. After exposure, the sheet samples were cut open and inspected for moisture. In addition to hydrophobic coating performance, the samples were also studied for flexibility of coating material, durability of coating material, and required coating thickness.

Within the second investigation, PBO strands of similar length were pulled from woven Zylon sheets and investigated for physical properties including filament diameter, changes in dimension (diameter and weight) when exposed to water, and the variations in tensile strength due to exposure to water. The filament quantity and physical size were measured using a Scanning Electron Microscope (SEM). For tensile testing, the cross-sectional area of the filaments (approximately 30 strands per sample) was measured using the SEM and the combined area of the filament set was inputted as the cross-sectional area. As the published elongation of Zylon was 2.5%, the active area of the filaments applied to tensile testing was approximately 23 centimeters.

Lastly, a  $V_{50}$  assessment was conducted to determine the velocity at which projectile penetration was 50%, using a light gas gun to fire 0.952 cm chromium steel spheres at both coated and uncoated Zylon samples, both serving as controls (no water

exposure) and submerged water exposure for 96 hours at a set temperature. In all ballistic studies, the loading on the fibers was measured through the incorporation of strain gauge load cells in the x- and y-directions.

**B. HYDROPHOBIC COATING TRIALS**

The hydrophobic coating used on the Zylon samples during the V<sub>50</sub> assessment needed to be durable but flexible, without adding unnecessary bulk to the characteristically lightweight fabric, in addition to creating a waterproof barrier between the environment and the PBO. Twelve coatings were selected for testing, including both spray and brush applications, listed in Table 1. Seven coatings were commercially available within hardware/home repair retail outlets. The additional five coatings were industrial-grade and acquired through Kraton Corporation. It should be noted that the Kraton polymers arrived in solid pellet form and required dissolving within xylene to enable liquid application.

Table 1. List of tested commercial and industrial grade hydrophobic coatings.

<b>Commercial Grade</b>	<b>Industrial Grade</b>
Flex Seal Liquid Coating (clear)	Kraton FG1924 Polymer
HERCO Fish Pond Neoprene (black)	Kraton MD1653 Polymer
Creature Cast Super Flex Rubber (black)	Kraton MD6951 Polymer
Thermoplastic (white)	Kraton MD1648 Polymer
Flex Seal Spray (clear)	Kraton G1657 Polymer
Plasti Dip Spray (clear)	
Leak Seal Spray (white)	

Each sample in the hydrophobic coating trials was made of 20 cm by 20 cm squares of woven cotton fiber sheets approximately 0.2 mm thick, with five sheets per sample for a thickness of 1 mm. The center (third) sheet of fabric was marked with 3M water contact indicator tape. Nine contact indicators were placed on each corner, the middle of each edge, and the center of the fabric sheet, as shown in Figure 7. This process was repeated on the opposite side of the sheet for a total of 18 water contact indicators used in each test sample. When exposed to moisture, the water contact indicators turn red and bleed on to the fabric, which is demonstrated in Figure 8.

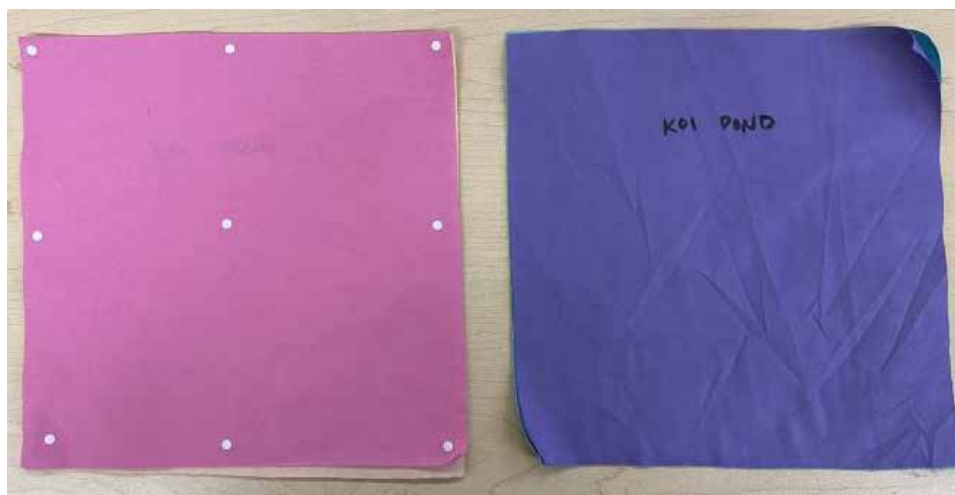


Figure 7. Water contact indicator placement on coating samples.

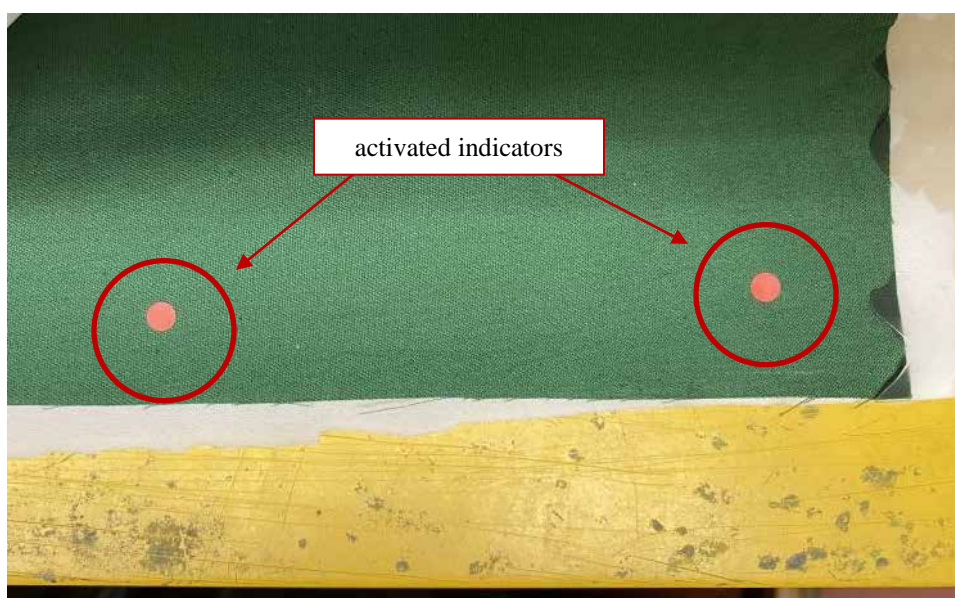


Figure 8. Activated water contact indicator stickers. Note the spreading of the red dye from the stickers due to moisture exposure.

Samples were coated one side at a time to allow for complete drying. Liquid coatings required only one application per side provided that there were no gaps in the coating due to errors in the application process. Spray coatings required three applications per side to ensure that the entire surface of the sample was covered. Spray coatings and the thinner liquid coatings also required a method of keeping the edges of the fabric samples

together during application, as these coatings were of insufficient thickness when dry to hold all five layers together. This was accomplished mainly through the use of masking tape folded over the edges, as seen in Figure 9.



Figure 9. Placement of tape around edges of coating sample.

Once coatings were applied to both sides of the sample, the samples were placed in a moisture-rich environment simulated by a fog chamber apparatus (ASTM B-117), shown in Figure 10, at 35°C for a period of 48 hours. Although the apparatus is capable of holding saltwater, only distilled water was used for this experiment. Due to limited space within the chamber, samples were placed in batches of up to four different coatings. The coatings tested in each set are listed in Table 2.



Figure 10. Fog chamber apparatus.

Table 2. Waterproof coating sample sets.

Set	# of Samples	Sample Details
1	4	HERCO Fish Pond Neoprene, Creature Cast Super Flex Rubber, Thermoplastic, Flex Seal Liquid Coating
2	3	Flex Seal Spray, Plasti Dip Spray, Leak Seal Spray
3	2	Flex Seal Spray
4	2	Flex Seal Liquid Coating, Flex Seal Spray

<b>5</b>	3	MD6951 (25/75 ratio by weight), MD1648 (25/75), MD1653 (25/75)
<b>6</b>	3	MD6951 (50/50), MD1648 (50/50), MD1653 (40/60)
<b>7</b>	2	G1657 (45/55), FG1924 (40/60)
<b>8</b>	4	Flex Seal Liquid Coating, MD6951 (50/50), MD1648 (60/40), G1657 (30/70)

Upon completion of the 48-hour exposure period, samples were removed from the fog chamber apparatus and allowed to sit at room temperature for 12 hours. This was done to encourage drying on the surface of the samples, to avoid contaminating any untouched water contact indicators once the sample was cut open. Once the sample was dried, the coating was cut open, and coating thickness measurements were taken for multiple locations both sides of the sample with a caliper. The number of water contact indicators that showed moisture intrusion were noted, as well as if the fabric was damp inside of the coated sample.

### C. ZYLON TENSILE TESTING

The given tensile strength for Zylon (5.9 GPa) needed to be verified experimentally prior to the  $V_{50}$  assessment, where the coating applied to the woven sheets of PBO or the frames they are mounted on may affect their material properties. The PBO filaments tested in lengths of 35 cm in groups of approximately thirty strands removed from an as-received Zylon weft group. Each sample was a part of a set prepared in differing criteria detailed in Table 3. A 0.635 cm piece was taken from each sample and attached to a slide, shown in Figure 11.

Table 3. Zylon tensile test sample sets.

<b>Set</b>	<b># of Samples</b>	<b>Sample Details</b>
<b>1</b>	5	Zylon with no waterproof coating, unexposed to moisture
<b>2</b>	5	Zylon with no waterproof coating, exposed to moisture for 96 hours
<b>3</b>	5	Zylon with waterproof coating, unexposed to moisture

4	5	Zylon with waterproof coating, exposed to moisture for 96 hours
---	---	---

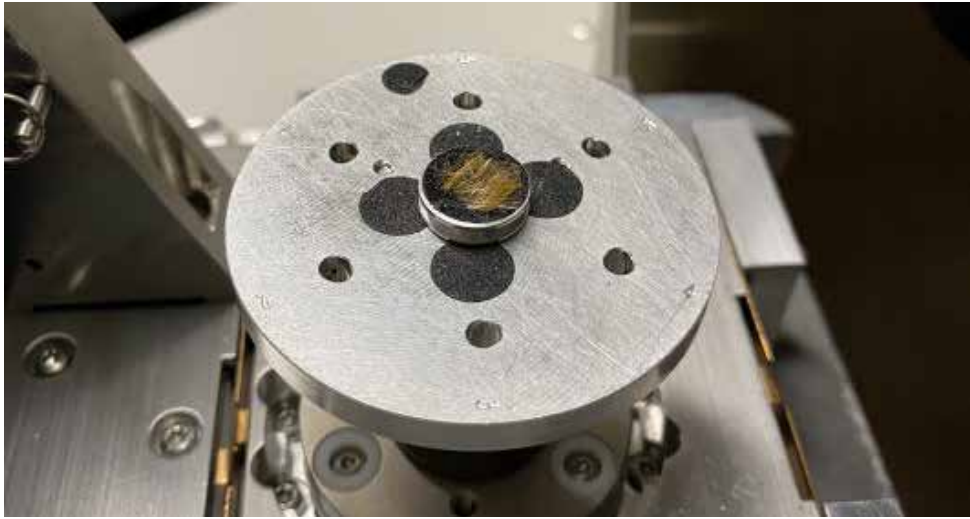


Figure 11. Zylon sample on a scanning electron microscope slide.

The slide was then placed in a scanning electron microscope (SEM) for baseline analysis, as seen in Figure 12, to count the exact number of strands in each sample as well as take photos and measure the width of each individual strand. An SEM accelerates electrons in a vacuum chamber through a column of lenses and apertures to create a concentrated, scanning beam on to the sample. Sensors detect the reflected electrons and enable correlation of the reflected electrons to construct an image of the probed target material.

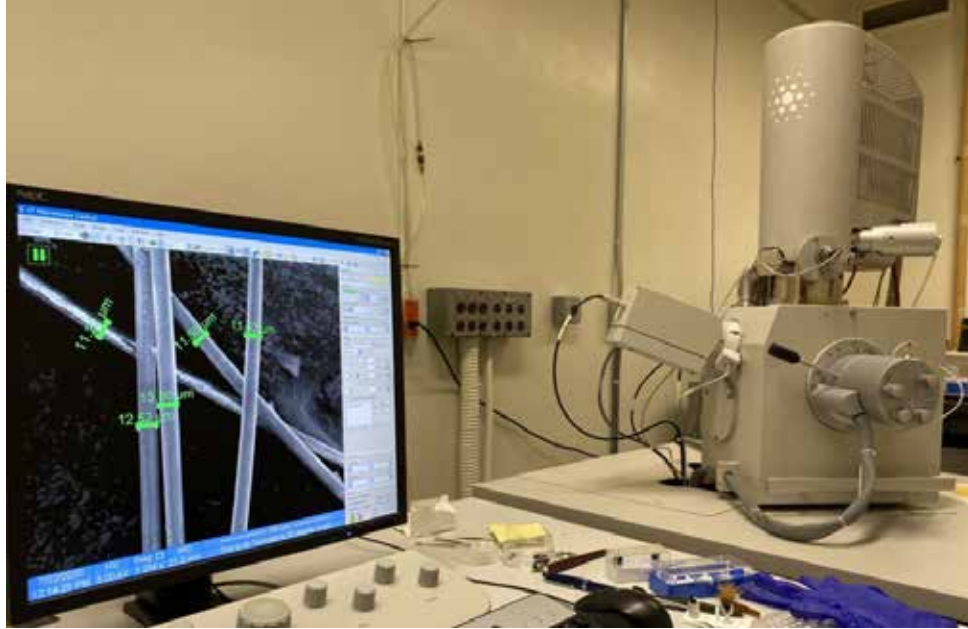


Figure 12. Taking strand measurements utilizing the scanning electron microscope.

The thickness of each sample was obtained from these measured widths using the equation

$$A_x = \sum \pi(w/2)^2 \quad (2)$$

where  $A_x$  is the cross-sectional area of the sample and  $w$  is the width of each strand. The remainder of the 10-inch samples were wrapped at both ends around a 0.318 cm wooden dowels cut into lengths of 5 cm each and affixed with black Gorilla Tape, shown in Figure 13. This was done to ensure the teeth in the mounting frame of the Instron tensile testing machine did not cut into the PBO fiber, while also providing a measure of grip on the sample. All wrapped samples were measured to approximately 7.62 cm in length. Samples were mounted in the Instron model 1000 (Figure 14), with attached load cells used to collect data via a National Instruments USB data acquisition system into a separate LabVIEW program, which utilized the cross-sectional area computed in Equation 2 to graph the stress-strain curve of the PBO.

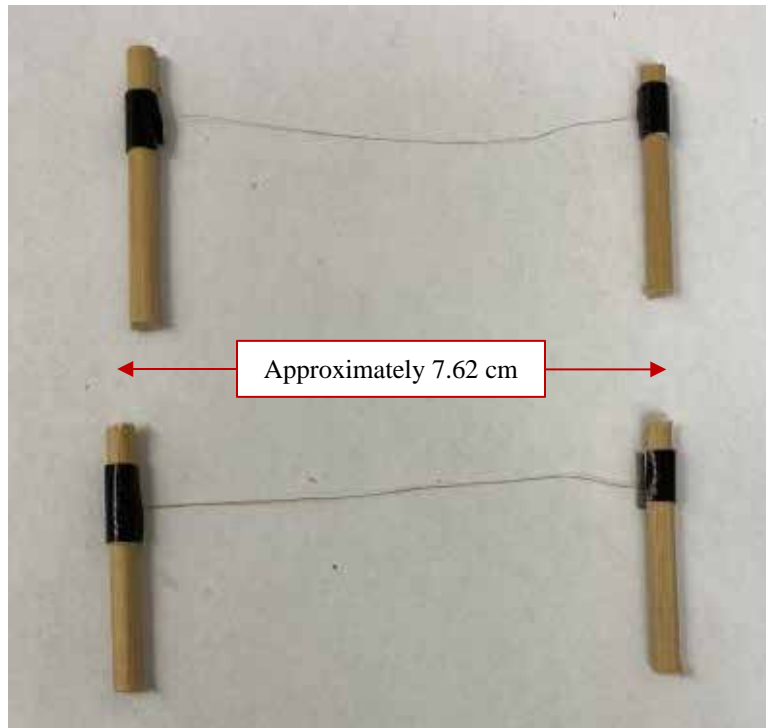


Figure 13. Zylon samples prepped for tensile testing.



Figure 14. Instron tensile testing machine with attached load cell for elongation measurements.

The PBO fiber sample was then subjected to tension, increasing the vertical distance between the two mounts at 1.7 mm/min. Stress-strain data was monitored in real-time to assess the sample until first-strand breakage, providing the ultimate tensile stress of the sample.

#### **D. $V_{50}$ ASSESSMENT**

The  $V_{50}$  assessment was performed using a Physics Application Incorporated 25.4 mm smooth bore light gas gun, which can launch projectiles of over 1100 m/s. The light gas gun includes two air compressors (a 150 psi screw-type air compressor feeding a 6000 psi compressor), control system, regenerative breech system, 4-meter-long gun barrel, and blast tank. The system can be seen from the breech to the catch tank in Figure 15.



Figure 15. Breech, barrel, and catch tank of the light gas gun.

A National Instruments PXI data acquisition chassis and installed LabVIEW program are used to control filling, venting, and firing of the gun through a series of electro-pneumatic valves, shown in Figure 16.



Figure 16. Valve and firing control system for the light gas gun.

The projectile used was a 0.952 cm chromium steel sphere housed in a four-piece serrated sabot 3-D printed out of solid polycarbonate and machined to fit in the gun bore, shown in Figure 17. The sabot's 45-degree internal angle allowed it to aerodynamically separate and strip away from the chromium sphere upon exiting the muzzle, ensuring that only the sphere strikes the sample. A steel stripper plate with a 10 cm aperture assists in separating the sabot and the sphere, as well as protecting the sample from the majority of sabot shrapnel.

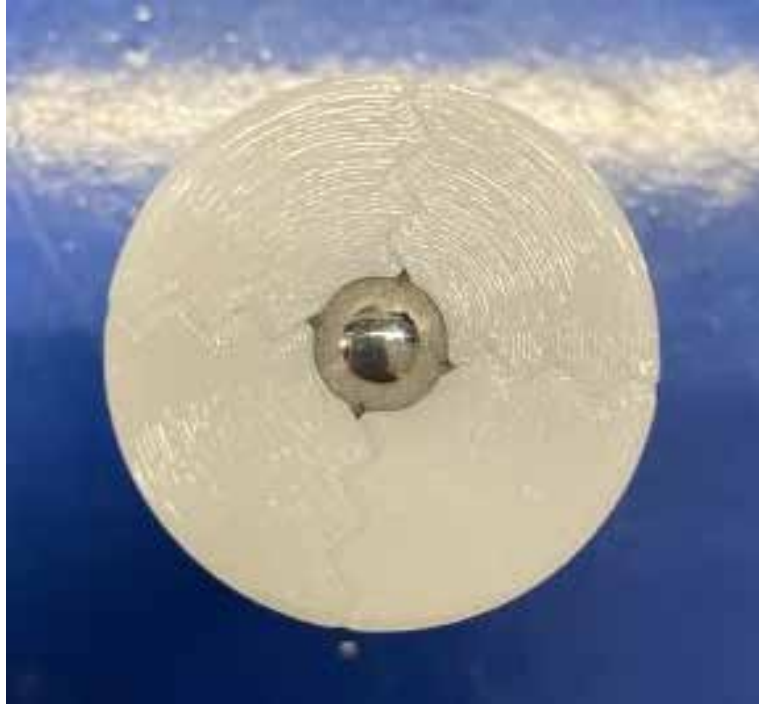


Figure 17. Chromium steel sphere and four-piece serrated sabot.

The Zylon samples were created from two 35 cm by 8 cm woven strips, the first held vertically lengthwise and the second offset by  $90^\circ$  to be held horizontally lengthwise. Each weft is attached to a load cell in the y- and x-direction, respectively. The sample and load cells are arranged in a steel frame 45 cm by 45 cm that slides into the catch tank at the end of the light gas gun and can be bolted down for stability. This frame and a Zylon sample can be seen in Figure 18. Each sample was a part of a set prepared in differing criteria detailed in Table 4. For standardization purposes, the first layer of Zylon weft was always placed in the y-direction, while the second layer was always placed in the x-direction.

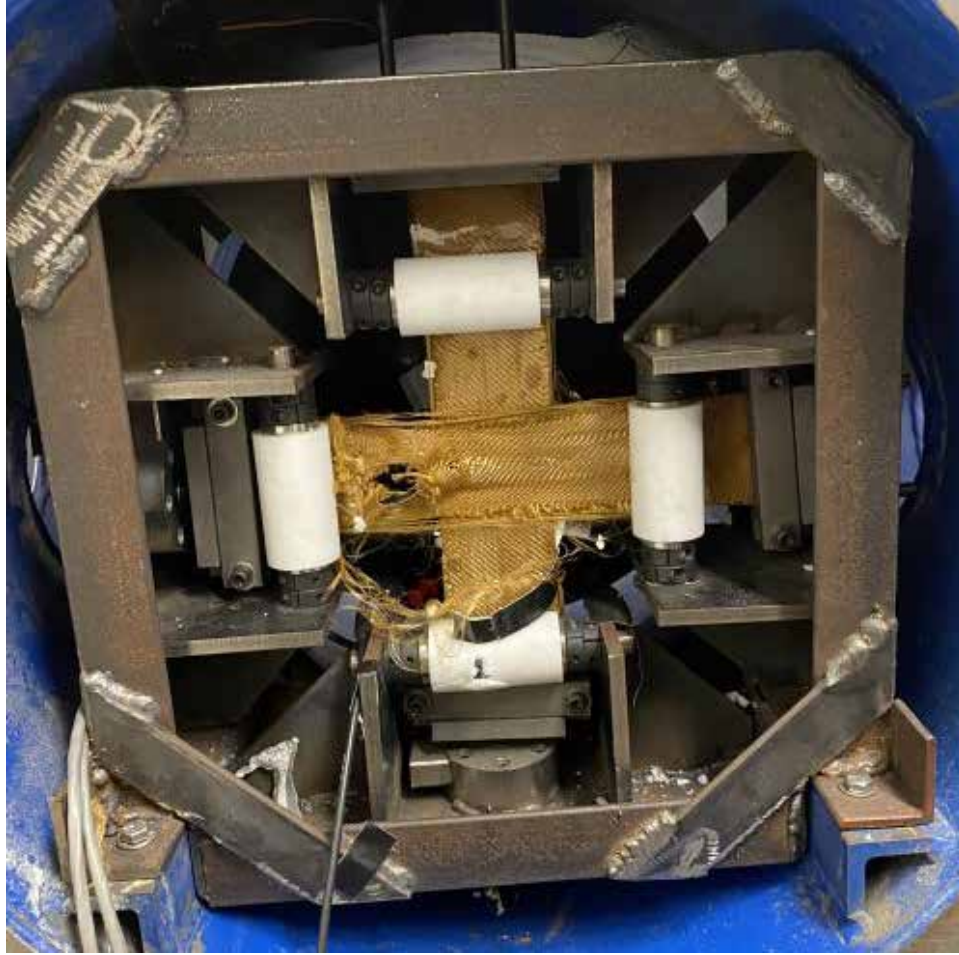


Figure 18. Frame with uncoated, unexposed Zylon weft sample, post-shot.

Table 4.  $V_{50}$  assessment sample sets.

Set	# of Samples	Sample Details
1	24	Zylon with no waterproof coating, unexposed to moisture (control)
2	9	Zylon with no waterproof coating, exposed to moisture for 96 hours
3	15	Zylon with waterproof coating, unexposed to moisture
4	3	Zylon with waterproof coating, exposed to moisture for 96 hours

Sample data acquisition is handled via a different LabVIEW program which collects data from load cells attached to the sample frame in the catch tank, shown in Figure 19. The two load cells attached to the sample act as force transducers, converting the tension forces enacted by the projectile on the textile sample into an electrical signal read by the

LabVIEW program. When the tension force increases on the sample, the corresponding signal changes proportionally. Due to adjustments on the frame, zero values for each of the load cells may differ from sample-to-sample and were noted prior to each test shot.

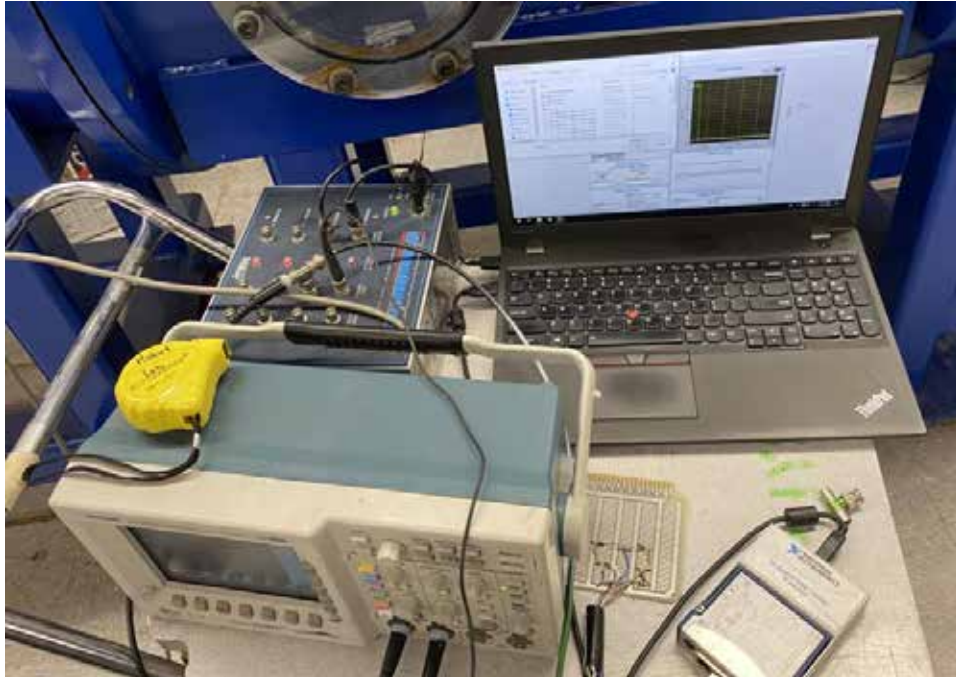


Figure 19. Data collection system for the light gas gun.

Break screens were attached to both the center of the sample frame (Figure 20) and placed over the aperture of the sabot stripper plate (Figure 21). A Whithner Triggerbox 1000 was used to create a 10 V square pulse when the break screen conductivity was broken. Using the known distance between the two break screens (0.368 m) and the measured time between pulses (measured by a Tektronix TDS 3034B four-channel oscilloscope), the velocity of the projectile could be determined. Shots fired ranged from about 150 m/s to 400 m/s over all sample sets, corresponding to pressures of 50 psi to 500 psi.

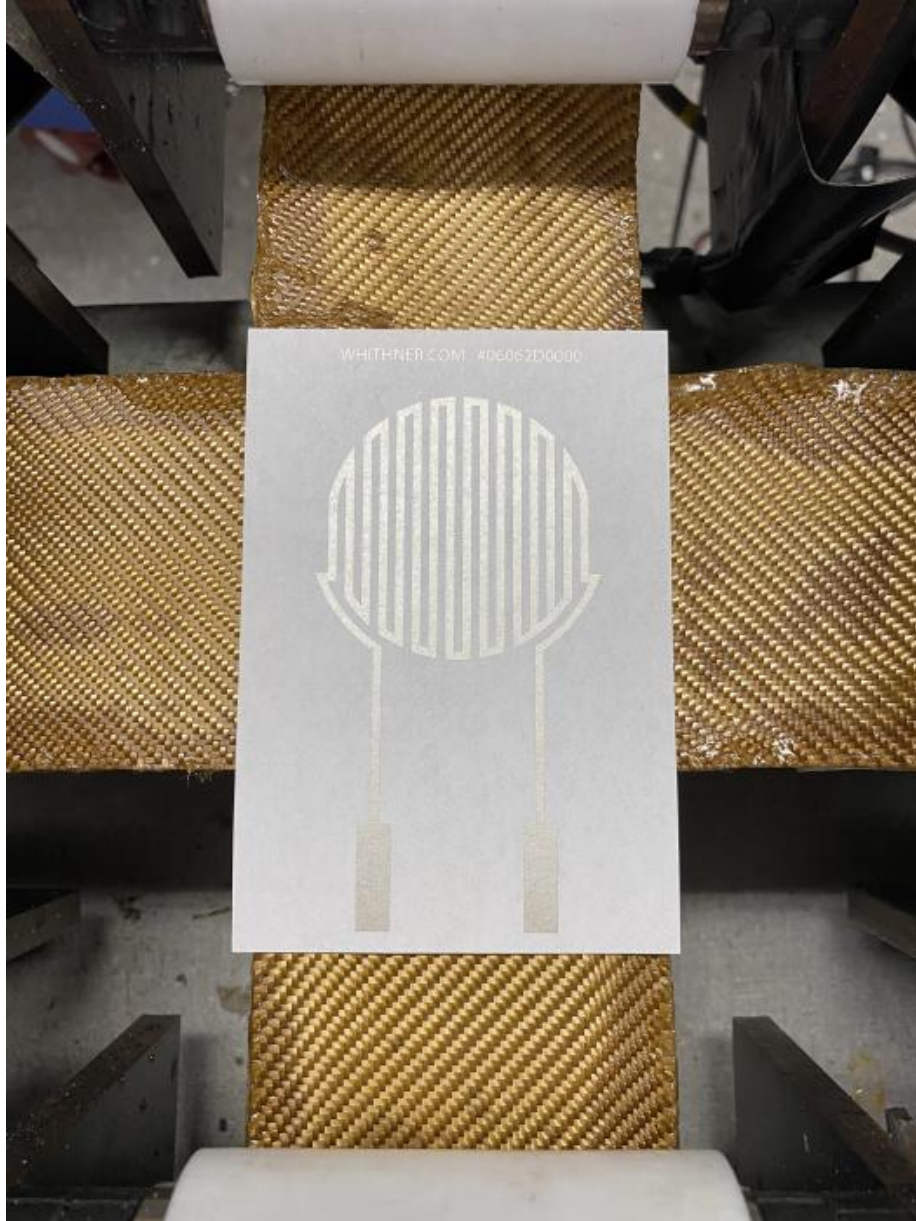


Figure 20. Placement of the break sheet on the center of the sample wefts.

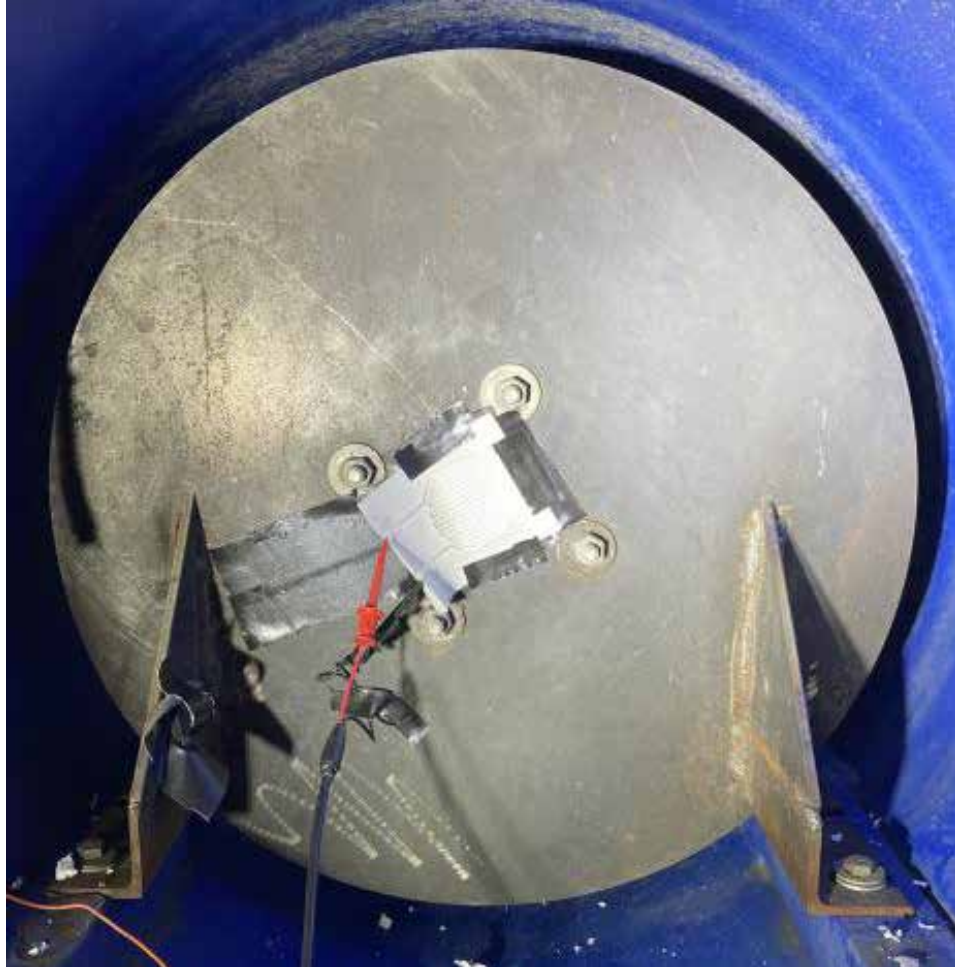


Figure 21. Placement of the break sheet on the stripper plate.

Two methods were used to verify sample penetration: a simple backing, and high-speed image capture. Two pieces of 8 cm wide Gorilla Tape were placed across the back of the sample frame in corresponding directions and locations to the sample, as shown in Figure 22. Any projectile which penetrated the sample should also penetrate this “backing” tape, providing a form of visual identification. In addition, a Vision Research Phantom v2512 high-speed video camera (Figure 23) was used to capture a collection of 400 x 250 32-micron pixel resolution images of each sample test at 1,000,000 frames per second. The camera was triggered by the second break screen located in front of the textile sample system. With a short exposure time of less than 100 ns, two high-intensity “7-UP” LED lights were used to furnish adequate lighting during the image capture.

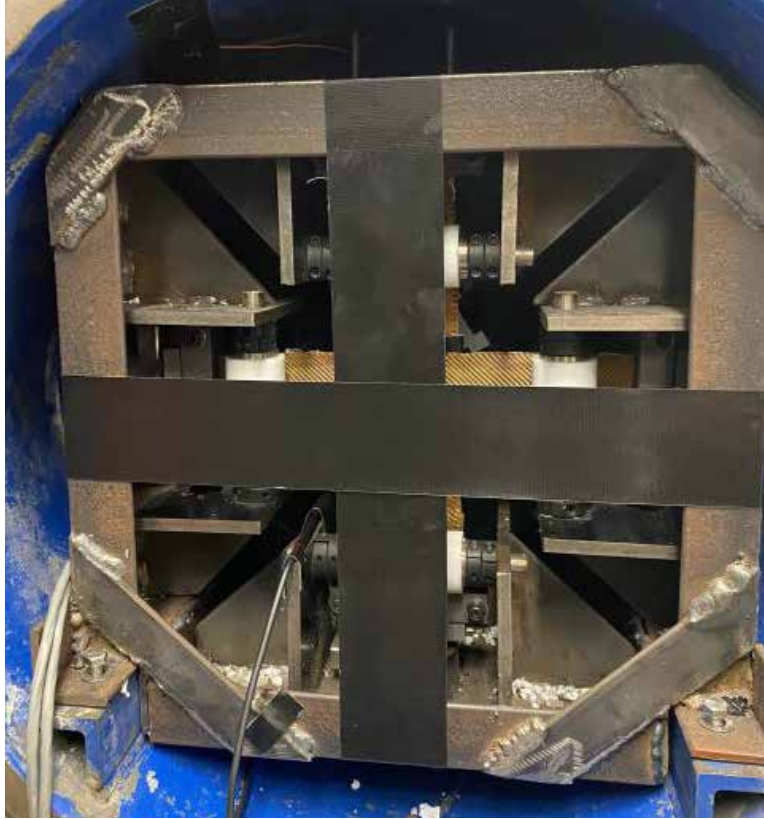


Figure 22. Placement of backing tape behind the sample wefts.



Figure 23. Camera and lighting setup for experiment image capture.

As the catch tank would remain open and unbolted for the camera to witness the sample test, two 60 cm diameter, 3 cm thick clear polycarbonate plates with a 1.27 cm–thick steel plate were placed behind the sample frame and bolted in place, seen in Figure 24, to prevent escape of the projectile after a complete penetration.



Figure 24. Clear polycarbonate plates attached to catch tank.

Upon completion of each test shot, the catch tank was disassembled, and the sample removed from the frame for analysis. Velocity was calculated from the time between the two break screen penetrations (distance 0.368 m), as detailed earlier. High-speed imaging and the sample's backing tape were inspected for evidence of complete sample penetration. In the case of partial sample penetration, collected load cell data was checked for a clear difference in pressure between the two layers.

## IV. DATA

All data from the experimental research will be expressed in SI units. The penetration velocity of the  $V_{50}$  assessment is the only exception, using feet-per-second (ft/s) due to standard convention in the armor community.

### A. HYDROPHOBIC COATINGS RESULTS

#### 1. COMMERCIAL OFF-THE-SHELF COATINGS

The purpose of the hydrophobic coating trials was to find a coating solution for PBO that is thin, flexible, easy to apply, and above all, waterproof. Coatings chosen for testing were either COTS products or industrial-grade polymers dissolved in xylene. Coating trials were performed in sets, for a total of 24 coated fabric samples divided into 8 sets: 4 sets focusing on the commercial coatings, 3 sets focusing on industrial coatings, and 1 set comparing the best of both. The first 4 sets of data for commercial coatings can be found in Table 5.

Table 5. Commercial off-the-shelf coating data sets.

Set	Coating	Coating Detail	Coating Thickness (mm)	Activated Indicators (X / 18)
1	HERCO Fish Pond Neoprene	Black	0.42804	18
1	Creature Cast Rubber	Black, Super Flex	0.19436	18
1	Thermoplastic	White	0.11816	18
1	Flex Seal	Liquid	0.72268	7
2	Flex Seal	Spray	0.26990	4
2	Plasti Dip	Spray	0.09845	18
2	Leak Seal	Spray	0.39436	14
3	Flex Seal	Spray	0.14036	18
3	Flex Seal	Spray	0.05908	18
4	Flex Seal	Liquid	0.71760	0
4	Flex Seal	Spray	0.19116	18

The coatings analyzed for Set 1 were treated as an initial sampling for types of commercial coatings used for different waterproof or water-resistant applications. Although it was somewhat effective, the liquid Flex Seal was almost twice as thick as the second thickest coating in Set 1 (HERCO Fish Pond neoprene). To reduce the coating thickness while keeping the same effectiveness, products similar to Flex Seal, but with an aerosol application rather than a liquid form, were chosen for the coatings used in Set 2. The Flex Seal spray was further explored in Set 3, but neither sample had a coating thick enough (both were thinner than the previous Flex Seal spray sample) or even enough to ensure effective waterproofing. Set 4 compared the Flex Seal liquid to the Flex Seal spray.

## 2. INDUSTRIAL-GRADE COATINGS

As the Kraton polymers used in Sets 5 thru 7 needed to be dissolved in xylene, there was an opportunity for more control over the thickness of each coating. Technical consultation with Kraton representatives suggested started in a 25% to 75% weight ratio of polymer to solvent and adjusting based on required viscosity. The next 3 sets of data for commercial coatings can be found in Table 6.

Table 6. Industrial-grade coating data sets.

Set	Coating	Coating Detail	Coating Thickness (mm)	Activated Indicators (X / 18)
5	Kraton MD6951	25/75 (Polymer/Xylene)	0.42804	18
5	Kraton MD1648	25/75 (Polymer/Xylene)	0.27818	18
5	Kraton MD1653	25/75 (Polymer/Xylene)	0.56012	18
6	Kraton MD6951	50/50 (Polymer/Xylene)	0.6414	0
6	Kraton MD1648	50/50 (Polymer/Xylene)	0.5398	0
6	Kraton MD1653	40/60 (Polymer/Xylene)	0.997	0
7	Kraton G1657	45/55 (Polymer/Xylene)	0.4763	0
7	Kraton FG1924	40/60 (Polymer/Xylene)	0.6668	0

Set 5 used the 25/75 mixture recommendation for three of the Kraton polymers. The recommended 25%/75% weight ratio of polymer to solvent, however, was far too thin for use as a coating on the fabric samples. The mixture ratios for each coating were

recalibrated and the same polymers were used for Set 6, which were thicker and performed more to standard. Using similar mixture ratios to those in Set 6, two more Kraton polymers were tested in Set 7. As the polymers' stiffness would only increase with a greater ratio of polymer-to-solvent, they were not re-tested.

### 3. LEADING COATING TESTS

The final set of coatings analyzed the best products from the commercial and industrial-grade sets: Flex Seal liquid, Kraton MD6951, Kraton MD1648, and Kraton G1657. The data for Set 8 can be found in Table 7. While the Flex Seal spray could likely provide the same waterproofing properties as its liquid counterpart, the results of its application were too inconsistent to be considered reliable. A few adjustments were made to the mixture ratios for the Kraton polymer coatings to dilute or thicken the polymer based on prior sample sets.

Table 7. Leading coating data set.

Set	Coating	Coating Detail	Coating Thickness (mm)	Activated Indicators (X / 18)
8	Flex Seal	Liquid	0.70744	0
8	Kraton MD6951	50/50 (Polymer/Xylene)	0.6922	6
8	Kraton MD1648	60/40 (Polymer/Xylene)	0.5906	10
8	Kraton G1657	30/70 (Polymer/Xylene)	0.5144	13

### B. INSTRON TENSILE TEST RESULTS

A tensile test for the PBO fiber was required to verify the tensile strength of the material prior to the V<sub>50</sub> assessment. Bundles of 30 strands were pulled from woven sheets of Zylon and analyzed with a scanning electron microscope both before and after exposure to heat (50°C) and moisture for 96 hours to measure their widths and note any visual differences. After, the samples were attached to an Instron machine and subjected to tension. Results from the initial 3 samples are shown in Table 8. Samples clearly showed an increase in width for each of the strands, also seen in Figures 25 and 26.

Table 8. Initial PBO sample SEM and Instron data. PBO was exposed to heat and water for 96 hours.

Sample	Sample Parameters	# of Strands	Cross-Sectional Area [Before] ( $\mu\text{m}^2$ )	Cross-Sectional Area [After] ( $\mu\text{m}^2$ )	Ultimate Stress (GPa)
1	PBO: 96-Hour, Heat-Exposed (50°), Water-Exposed	28	4.845	5.826	1.635
2	PBO: 96-Hour, Heat-Exposed (50°), Water-Exposed	26	4.385	5.172	1.403
3	PBO: 96-Hour, Heat-Exposed (50°), Water-Exposed	20	3.411	3.870	0.957

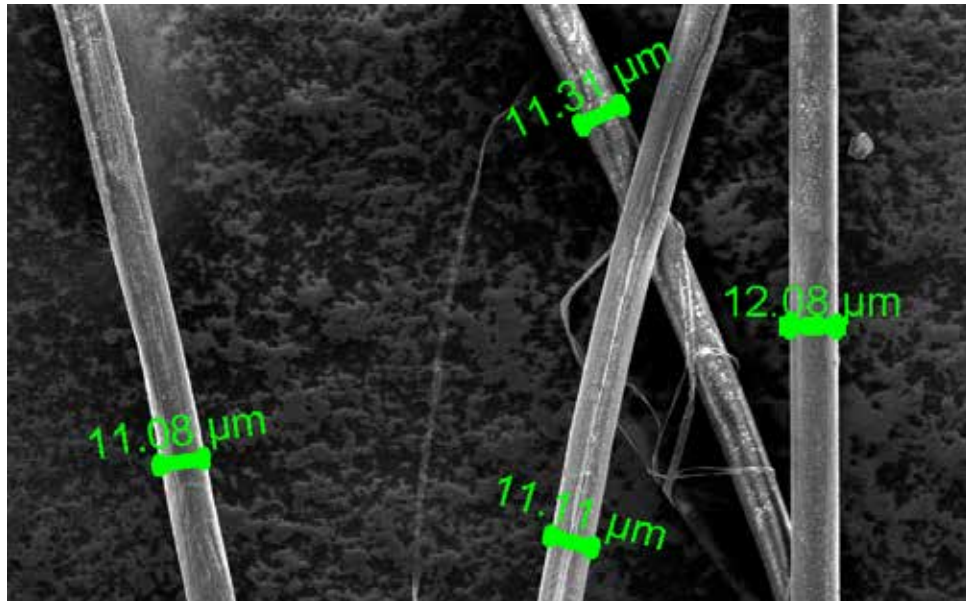


Figure 25. SEM width measurements of unexposed PBO fiber strands.

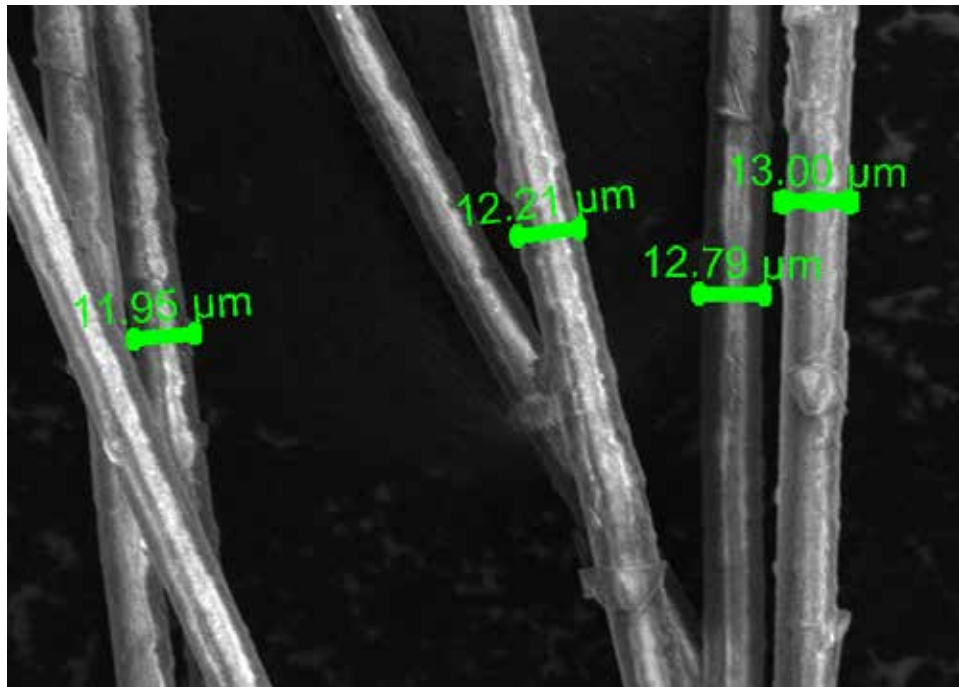


Figure 26. SEM width measurements of PBO fiber strands exposed to heat (50°C) and moisture for 96 hours.

The ultimate stress found for each of the samples was far below the expected value of 5.9 GPa. It is possible that strands in the samples were not secure enough to the dowels, registering a false “break” in the sample from a weak or displaced strand. To try and negate the error caused by splitting approximately 30 individual strands from the original Zylon weave, single strand samples were also attempted, as seen in Figure 27. This method, however, was difficult to pursue, as trying to handle single strands of PBO approximately 10–14 μm thick was unwieldy and resulted in over-handling, breakage, or loss of the strands.



Figure 27. SEM slide with individual PBO fiber strands.

Focus was then shifted in the opposite direction: instead of single strands, tensile tests were completed using entire wefts of PBO pulled from the Zylon weave (Figure 28). Wefts consist of approximately 300 strands of PBO, which would be inefficient to count and measure with the SEM for a single sample. To compare changes from exposure, the masses of the wefts were instead measured before and after exposure to moisture using a Mettler Toledo AB104-S analytical balance, pictured in Figure 29.



Figure 28. PBO fiber weft being separated from a Zylon woven sheet.



Figure 29. Mettler Toledo AB104-S analytical balance, used for measuring mass of PBO wefts.

Three sets of 10 wefts were prepared and tested with the Instron model 1000: uncoated unexposed, uncoated exposed, and coated exposed. Following issues with the Flex Seal coating chemically interacting with the PBO and caused it to snap under static tension (similar issues were not observed during the  $V_{50}$ , when material experienced dynamic tension). To avoid chemical interaction with the weft, coated samples were first wrapped with cellophane prior to coating and exposure to water for 96 hours. This procedure negated the need for a coated unexposed sample set. Tensile strength and elongation were collected for each sample, and the stress-strain curves shown in Figures 30 thru 32 plotted via a LabVIEW program using data taken from attached load cells. A summary of data for the three best samples from each sample set can be found in Table 9, and the stress-strain graphs for each sample set are shown in Figures 30–32.

Table 9. Instron tensile test results.

Sample #	Material	Sample Parameters	Weight Before Exposure (g)	Weight After Exposure (g)	Ultimate Stress (GPa)
1	PBO	Uncoated, Unexposed	0.0590	-	2.44
2	PBO	Uncoated, Unexposed	0.0588	-	1.99
3	PBO	Uncoated, Unexposed	0.0588	-	2.06
1	PBO	Uncoated, Exposed	0.0590	0.0625	1.91
2	PBO	Uncoated, Exposed	0.0589	0.0595	2.04
8	PBO	Uncoated, Exposed	0.0587	0.0596	2.02
7	PBO	Coated, Exposed	0.0593	0.0595	2.79
8	PBO	Coated, Exposed	0.0582	0.0583	2.49
9	PBO	Coated, Exposed	0.0588	0.0589	2.64

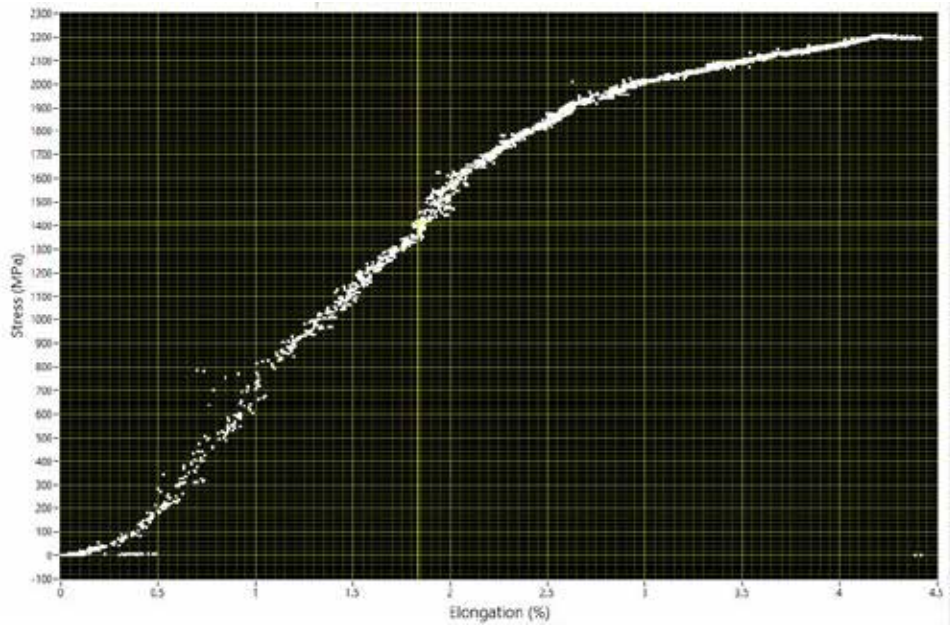


Figure 30. Stress-strain curve for uncoated unexposed PBO.

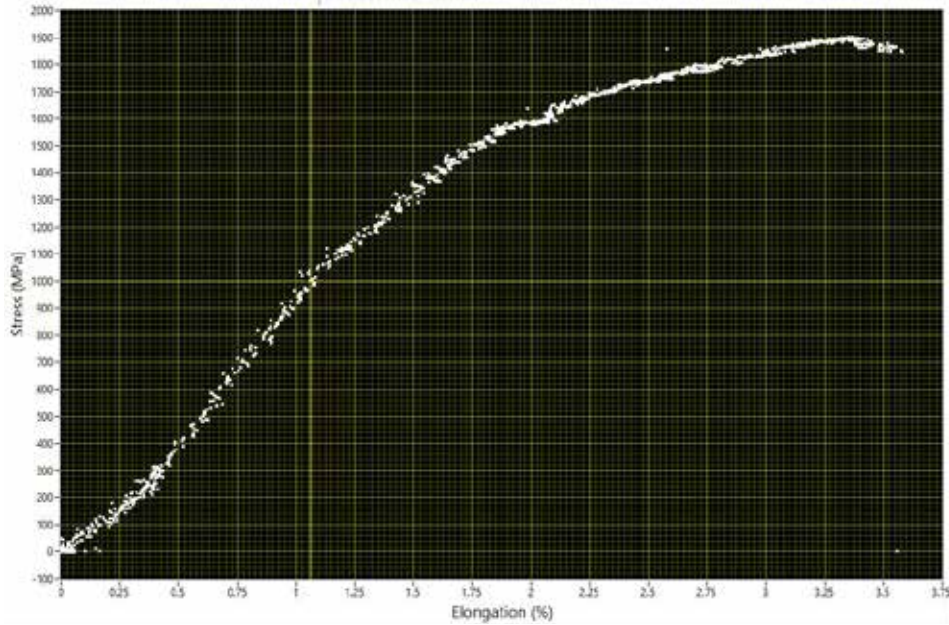


Figure 31. Stress-strain curve for uncoated exposed PBO.

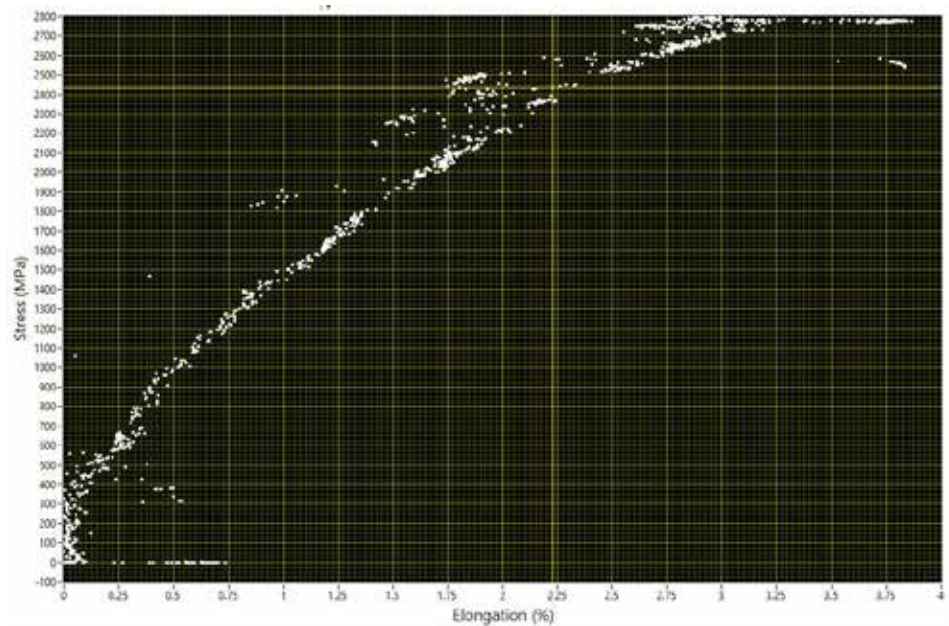


Figure 32. Stress-strain curve for coated exposed PBO.

Additional testing was done to see if PBO coated with the Kraton polymers or HMKV epoxy would display the same negative characteristics as those coated with Flex Seal. Three unexposed samples coated with Kraton G1657 and three samples coated with

HMVK were prepared and analyzed for indications of chemical reaction. They were then placed under tension in the Instron to measure their tensile strength. The results of this test are shown in Table 10.

Table 10. Additional coating tensile test results.

Sample #	Material	Sample Parameters	Ultimate Stress (GPa)
1	PBO	Coated with G1657, Unexposed	1.48
2	PBO	Coated with G1657, Unexposed	1.35
3	PBO	Coated with G1657, Unexposed	1.52
1	PBO	Coated with HMVK, Unexposed	1.24
2	PBO	Coated with HMVK, Unexposed	1.31
3	PBO	Coated with HMVK, Unexposed	1.07

### C. V<sub>50</sub> RESULTS

The V<sub>50</sub> assessment serves as a universal test for the performance of any ballistic fiber. Chromium steel sphere projectiles (0.952 cm in diameter) were fired at PBO fiber samples, adjusting in velocity until the difference between a partial penetration and a complete penetration was less than 50 ft/s, or 15.24 m/s. Four sample sets were tested as listed in Table 4. The number of samples per set was dependent on how many samples were needed to complete the V<sub>50</sub> as defined above. The partial and complete penetration velocities for each sample set are shown in Table 11. A full listing of each shot, to include firing pressure, time between break screens, and load cell offsets can be found in Appendix A. The resulting V<sub>50</sub> penetration velocity is found by averaging the partial and complete velocities found for each sample set.

Table 11.  $V_{50}$  penetration velocities for each PBO sample set.

<b>Material</b>	<b>Parameters</b>	<b>Partial Velocity (ft/s)</b>	<b>Complete Velocity (ft/s)</b>	<b><math>V_{50}</math> Penetration Velocity (ft/s)</b>
<b>PBO</b>	Uncoated, Unexposed	497.20	462.95	<b>480.08</b>
<b>PBO</b>	Coated, Unexposed	516.37	554.27	<b>535.32</b>
<b>PBO</b>	Uncoated, Exposed	539.42	468.33	<b>503.88</b>
<b>PBO</b>	Coated, Exposed	529.96	546.74	<b>538.35</b>

Load cell data was compiled and plotted over time in seconds for the partial and complete penetration velocity shots listed in Table 11, starting from the trigger of the second break screen to encompass the elastic wave (first wave) and returning plastic wave (second wave), in Figures 33 thru 36. “Vertical” load cell data corresponds to the first layer of PBO, while “horizontal” corresponds to the second layer of PBO.

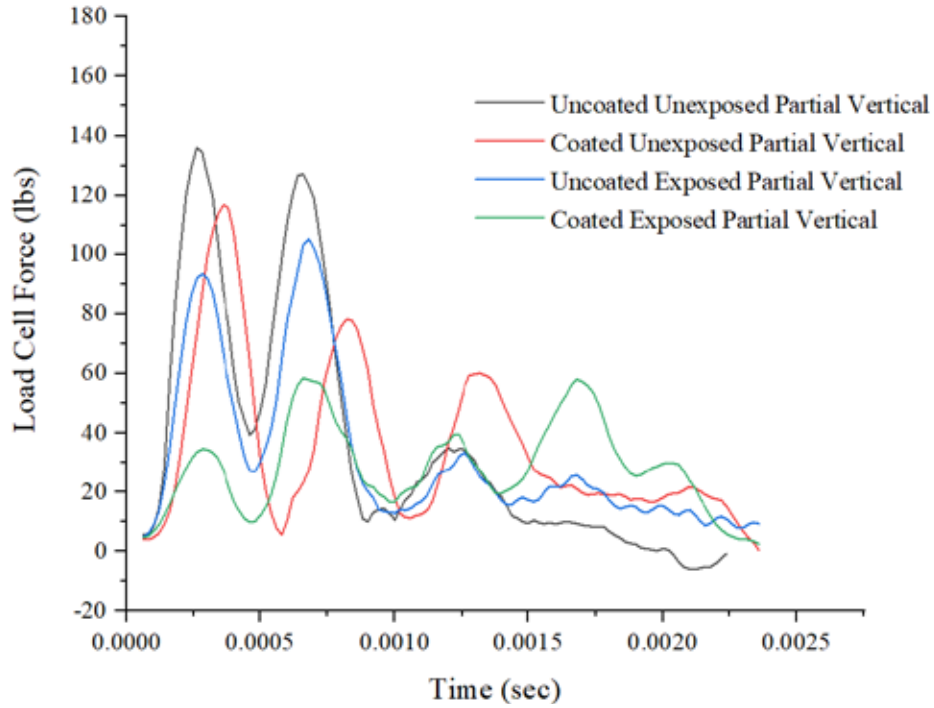


Figure 33. Vertical load cell data comparisons V50 partial penetration samples.

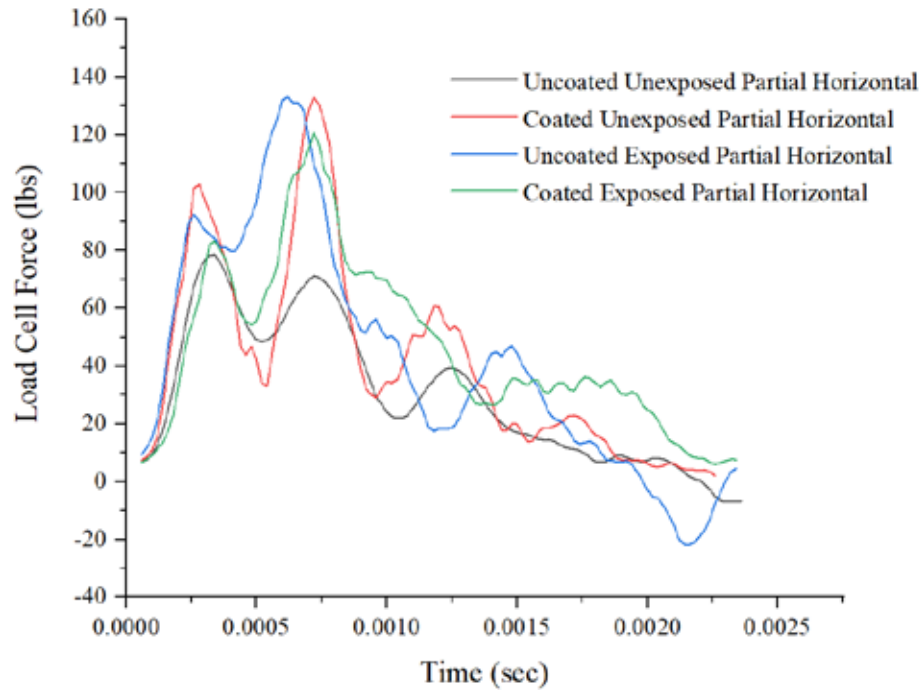


Figure 34. Horizontal load cell data comparisons V50 partial penetration samples.

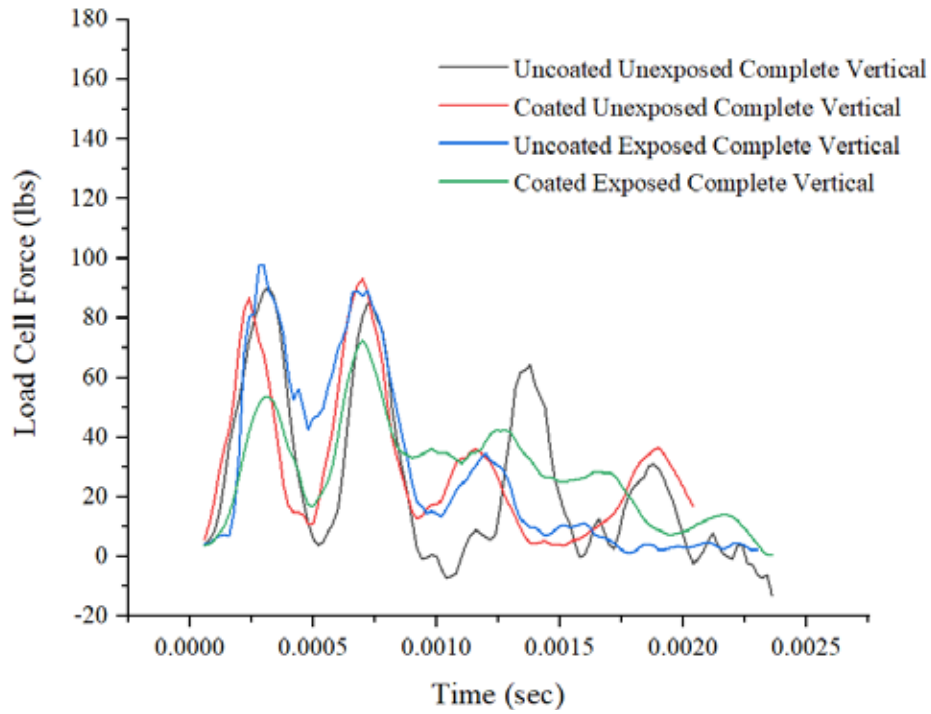


Figure 35. Vertical load cell data comparisons V50 complete penetration samples.

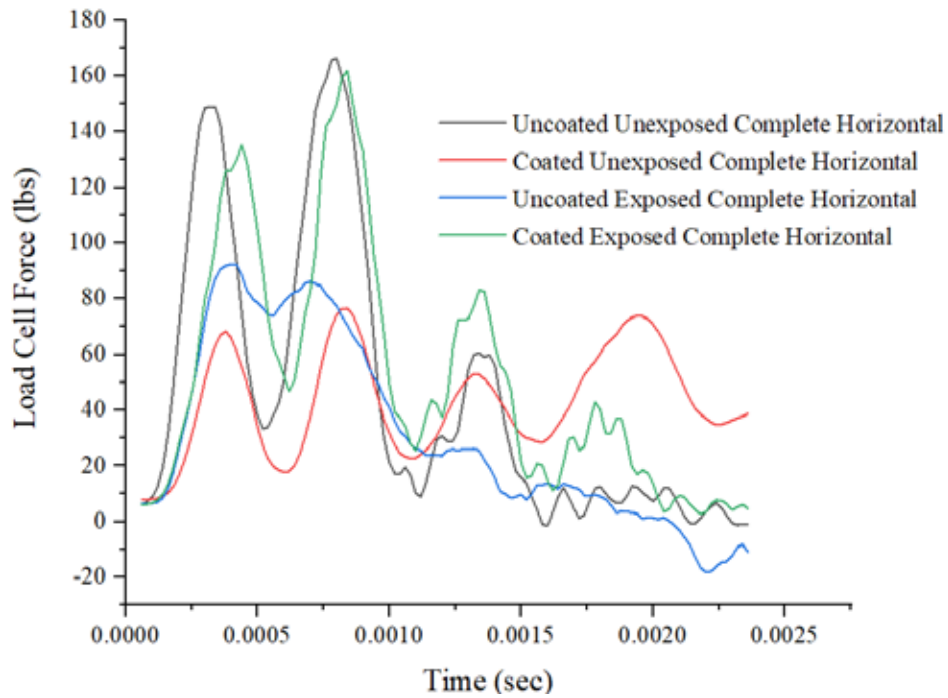


Figure 36. Horizontal load cell data comparisons V50 complete penetration samples.

THIS PAGE INTENTIONALLY LEFT BLANK

## V. DATA ANALYSIS

### A. HYDROPHOBIC COATINGS ANALYSIS

Between the Commercial off-the-shelf coatings and the industrial-grade polymers, the industrial polymers from Kraton undoubtedly performed more within to the desired parameters of a waterproof coating. The challenge, then, was that it was difficult to obtain consistent results regarding viscosity, set thickness, and permeability. Commercial coatings, despite their varying ranges of effectiveness in terms of hydrophobic performance, were simple in application and readily available.

While the HERCO neoprene, Creature Cast Rubber, and thermoplastic in Set 1 provided a thin, water-resistant shell to the fabric samples, when under sustained exposure the water permeated each of these coatings completely. The only coating that showed any sustained hydrophobic properties was the liquid Flex Seal, which was also the thickest coating used in Set 1 at 0.723 mm, as seen in Table 5. Upon further inspection the Flex Seal sample appeared to have experienced water intrusion via a small hole in the coating, resulting in 7 activated water indicators along one side.

To explore other options similar to Flex Seal but in aerosol form, two other options were appropriated for Set 2: Plasti Dip and Leak Seal. The Plasti Dip spray and Leak Seal spray did not achieve the same success as the Flex Seal spray, however, which appeared to out-perform its liquid counterpart, quantified in Table 5. The Flex Seal spray was also thinner than liquid Flex Seal at 0.270 mm, making it an attractive commercial alternative.

In Set 3, additional coating layers for the Flex Seal spray were applied to try and recreate the thickness of the spray sample for Set 2, but still fell short and resulted in all water indicators being activated. The Flex Seal liquid performed much better, completely sealing the sample and resulting in no activated water indicators. Although the Flex Seal spray appeared to be a thinner, more effective option, it was difficult to visually judge just how many layers needed to be applied, or even if the layer completely covered the sample. For the compressed timeline of this experiment, consistency in application and

performance was favored over thickness, resulting in liquid Flex Seal being the leading hydrophobic coating from the COTS products.

Set 5 saw exploration into the industrial-grade polymer coatings from Kraton Corporation. The resulting coatings were very thin and soaked completely through all layers of each fabric sample, shown in Table 6. It is unclear whether it was the prolonged exposure to unevaporated xylene in the coating or the ineffectiveness of the thin coating under sustained water exposure that led to completely activated water indicators for all three samples.

The coatings in Set 6, while approximately twice as thick in the case of the MD1648 and MD1653 with their adjusted mixture ratios, performed far better than they did in Set 5. There were no activated water indicators in any of the samples. The MD1648 mixture soaked through the fabric and solidified the layers of the sample together, as did the MD6951, though to a smaller extent. The MD1653, however, came out extremely thick and stiffened the sample considerably, making it impossible to bend without cracking the coating.

Set 7 used mixture ratios like those in Set 6 for two new polymers. Despite this, both the G1657 and FG1924 were relatively thin mixtures that soaked through the fabric of their samples. Although neither resulted in activated water indicators, both samples were thick and somewhat stiff, especially the FG1924.

Of the 12 coatings used in the initial 7 sets, 4 were chosen for Set 8: Flex Seal liquid, MD6951, MD1648, and G1657. They were selected due to their hydrophobic performance and flexibility. The Kraton polymers, however, experienced some water indicator activation prior to being intentionally exposed to water, seen in Table 7. It is possible that the xylene in the Kraton coatings was not fully dissolved and, in its unevaporated form, activated the water indicators. It is also possible that during the time required for the Kraton to dry, it was exposed to moisture in the air that permeated the coating before it was fully set. This poses a concern for the application of the Kraton polymers, and if the xylene used to dissolve them will chemically interact with the PBO to weaken it, similarly as if it were exposed to moisture.

Although the Flex Seal was subject to the same application environment, it did not experience water indicator activation. In addition, liquid Flex Seal does not appear to activate the water indicators despite direct contact. All coated PBO samples during the Instron tensile tests and V50 assessment use liquid Flex Seal as their coating, with Flex Seal spray applied to any visible area that has been missed (along sample edges, or from air bubbles in the main coating).

## **B. INSTRON TENSILE TEST ANALYSIS**

As seen in Figures 25 and 26 and Table 9, there are multiple examples of visual and computational evidence towards a significant chemical change in high modulus PBO when exposed to moisture, despite the lower moisture regain of 0.6%. Cross-sectional area increases by approximately  $0.035 \mu\text{m}^2$  per strand, but mass increases minimally per strand (less than 0.0001 g). However, after exposure to water the PBO wefts felt stiff and brittle to the touch, becoming kinked when handled and individual strands easily snapped in-hand with a small amount of tensile force. This is further supported by the higher elastic modulus of the uncoated exposed PBO, shown by the slightly steeper slope of the stress-strain curve in Figure 31, which indicates a more brittle material.

True verification of tensile strength could not be conducted with the equipment at hand due to possible sample slippage when placed in the Instron. This was also likely caused from human error in the making of samples, resulting the PBO wefts not being properly secured to the wooden dowels. Results, however, remained self-consistent throughout testing between the uncoated and coated samples, averaging an ultimate tensile stress of about 2.08 GPa for uncoated, 2.64 GPa for coated, and 2.26 GPa overall. Due to the technique of wrapping the samples around a wooden dowel, a false elongation was observed, typically averaging approximately 1%. For this reason, only the ultimate tensile stress values were published.

There was a strong skew in ultimate tensile stress towards the coated samples by over 0.5 GPa, though the PBO samples were wrapped in cellophane and not exposed directly to either moisture or Flex Seal. A possible explanation is that the wefts may have been processed from different conditions and later integrated into the woven fabric. This

variation was observed where different wefts using the same wrapping conditions produced variations in tensile strength as much as 20%.

There were also indications of a chemical reaction between the PBO and the Flex Seal coating, as well as with the Kraton G1657 coating and HMVK epoxy. At least in static tension the stiffening of the PBO caused by the coatings appear to weaken it, with the average tensile strength of these direct-coated samples being 1.33 GPa (Table 10), 0.75 GPa less than uncoated PBO.

### **C. V<sub>50</sub> ASSESSMENT ANALYSIS**

Overall, the velocities from the V<sub>50</sub> assessment were not as expected, though most of the behavior correlated from video evidence and load cell data corresponds to expected behavior for a partial and complete penetration of the fabric, respectively.

In a partial penetration, most of the projectile's kinetic energy is dissipated as the first layer of fabric arrests the projectile and increases the time it takes to penetrate it. By the time it reaches the second layer, the projectile's velocity and thus kinetic energy has significantly decreased, stopping it fully. This leads to a higher force on the load cell in the first layer of fabric (vertical load cell), and a diminished force on the load cell in the second layer of fabric (horizontal load cell). In a complete penetration, however, the higher velocity and kinetic energy are enough to penetrate the fabric before it can sufficiently arrest the projectile, resulting in similar forces on both the first and second layers.

It is also important to note that the deflection of the fabric caused by the projectile does not directly correspond to the peaks in force on the fabric. As seen in Figure 37, where the "tent" formed by the projectile on to uncoated, unexposed PBO is at its greatest deflection, time after trigger is 80  $\mu$ s and the horizontal load cell registers a force near base value (6.925 lbs, where base value is 6.25 lbs). The greatest force registered by the horizontal load cell (90.218 lbs) is long after the projectile has completely penetrated both layers, as the fabric is subject to elastic forces, shown in Figure 38.



Figure 37. Moment of peak deflection for uncoated unexposed PBO.

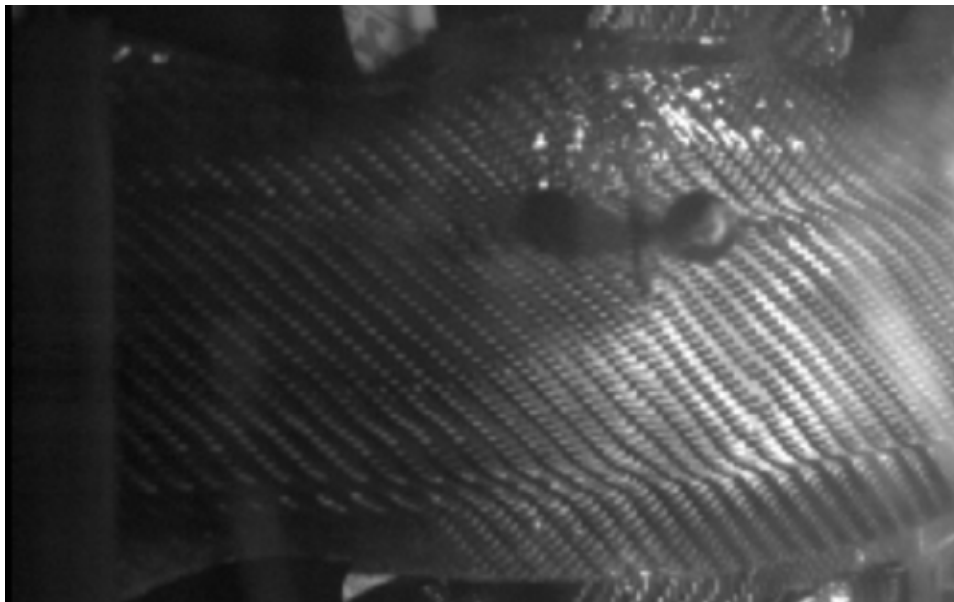


Figure 38. Moment of peak force on second layer of uncoated unexposed PBO. The projectile has already exited the sample.

While most of the data lends itself to this behavior, the load cell data depicted in Figures 33 thru 36 do not; the forces on the coated exposed PBO for both partial and complete penetration appear to be lower for the first layer, and significantly higher for the second layer. Although there is no conclusive reason as to why this occurred, it may be due to a chemical reaction between the Flex Seal and the Zylon, similar to what was observed on a smaller scale during the Instron tensile testing.

Aside from this, the uncoated exposed samples that experienced complete penetration see a merging of the two force peaks, shown in Figures 34 and 36. This may indicate a meeting of the elastic and plastic waves caused by the stiffening of the Zylon fabric when exposed to moisture. The stiffness of the fabric leads to a smaller deflection by a greater area of the fabric, making it more likely for the two waves to intersect.

The  $V_{50}$  penetration velocities themselves were also unexpected. The delta of 50 ft/s between partial and complete penetration velocities was meant to account for crossover and other approximations, as seen in Table 11 for the uncoated unexposed velocities with a difference of -28.23 ft/s. The crossover for the uncoated exposed velocities, however, is far greater than that, with a difference of -71.09 ft/s between partial and complete penetration velocities. As this is greater than the required delta of 50 ft/s, the skew may be caused by an outlying data point. The crossover is most likely explained by the degree of hygroscopic exposure to the PBO, resulting in variations in strength degradation.

That the partial penetration velocity of 539.42 ft/s for the uncoated exposed PBO is an outlying data point is further supported by the fact that according to this relatively high velocity, the uncoated exposed samples are stronger than those that have not been exposed. As seen in tensile testing, PBO becomes brittle when exposed to moisture for 96 hours. It is possible that the strength of a single weft differs from that of a woven sample, but it is also reasonable to assume that this would result in a lower penetration velocity than its unexposed counterpart.

The large disparity between the partial and complete penetration velocities of the uncoated exposed PBO aside, the  $V_{50}$  penetration velocities for the coated unexposed and

the coated exposed PBO are higher than those for the uncoated PBO. They are also relatively close to one another at 535.32 ft/s and 538.35 ft/s, respectively. This lends itself to the probability that the Flex Seal successfully protected the PBO from direct exposure to moisture, and even increased its  $V_{50}$  penetration velocity. Overall, it remains uncertain as to why such a large crossover in data regarding the uncoated PBO exists. Further research and additional data points are required to fully encapsulate the  $V_{50}$  penetration velocity, as well as identify and cull outliers.

THIS PAGE INTENTIONALLY LEFT BLANK

## VI. CONCLUSION

### A. OVERVIEW

Flex Seal liquid coating proved to be the most effective waterproof coating in terms of consistent hydrophobic performance, flexibility, and ease of application. Although its average coating thickness of 0.7159 mm is on the greater end of tested thicknesses, it remained consistent through multiple applications may be possible to achieve a thinner coating with specialty equipment. While the aerosol version of Flex Seal may provide a thinner, just as effective coating as its liquid counterpart, it is unclear how many layers are required to achieve complete waterproofing.

The investigated industrial-grade polymer coatings from Kraton Corporation achieved similar results but raised several concerns. Inconsistent coating thicknesses and setting times based on the mixture ratio between polymer and xylene made it difficult to predict their effect on samples. Mixtures with a higher weight ratio of polymer proved to be thick, stiff, and hard to apply; mixtures with a higher weight ratio of xylene bled through samples and took a long time to fully set, which may allow environmental moisture to penetrate the coating.

The Instron tensile test was unable to verify the stated tensile strength of Zylon, but ultimate tensile stress results of approximately 2.0 GPa were self-consistent across tested samples. SEM imaging, mass measurements, and tactile studies of Zylon strands before and after prolonged exposure to moisture indicated a chemical reaction between PBO and water. Strands appeared to gain mass and become more brittle, tending to snap in-hand when subject to minor tensile force. In addition, there appeared to be a chemical reaction occurring between the PBO strands and the coatings, to Flex Seal and Kraton G1657, stiffening the strands and causing them to snap when placed under static tensile load.

While the V50 assessment can be argued as inconclusive, results suggest that the Flex Seal coating provides a measure of additional strength to Zylon weave. Very similar V<sub>50</sub> penetration velocities between coated unexposed and coated exposed samples also support that the coating prevented the PBO from being exposed to moisture.

There were crossovers in the partial and complete penetration results for both uncoated unexposed PBO and uncoated exposed PBO. While the velocity crossover for uncoated unexposed PBO was minor and within the 50 ft/s variation provided between partial and complete penetration velocities, the crossover for uncoated exposed PBO was not. The reason for an over 70 ft/s difference between partial and complete penetration velocities for the uncoated exposed PBO is unclear, but the 539.42 ft/s partial penetration velocity is likely an outlier when compared to other results.

## **B. CHALLENGES**

It is important to note that designing PBO with a hydrophobic coating for use in ballistic armor is inherently a commercial problem. The methods used to conduct this research suggests that many issues which may plague the product down the line will most likely come from the manufacturing process—such as achieving an even thickness of coating, and identifying a method for stitching together coated PBO weave without ruining the integrity of the coating—and will require further study. It is not something that this research seeks to (or, in practicality, is able to) fully explore or duplicate, focusing instead on proving that PBO weave coated with hydrophobic substance retains its strength against high-velocity projectiles.

This was most clearly seen in the lack of specialty equipment at hand. With such a high tensile strength, cleanly slicing PBO weave requires a diamond laser cutter, which pushed back material shipping times and greatly limiting what shapes of the cut weave can be studied to what was provided by the supplier. Given the available setup of the measurement instruments attached to the light gas gun, which have been configured for unidirectional UHMWPE rather than a bidirectional PBO weave, a different or slightly altered method of quantifying a projectile's impact on the material was arranged. Having only one direction of the PBO weave under tension may have also affected the results of the  $V_{50}$  assessment and the fabric's overall performance.

In addition, due to the moratorium on using PBO as a ballistic fiber, it is difficult to obtain samples of the material for testing. Cotton fiber squares and UHMWPE samples of similar weight were used in preliminary experimentation and equipment calibrations to

avoid wasted PBO, especially during initial testing for coating effectiveness in high-moisture environments. The industrial coatings are also normally used in conjunction with industrial equipment such as sprayers and sanitary vent spaces during application to achieve a clean, even coat, but neither were readily available throughout experimentation. Measures were taken to not only replicate the thickness of each coating as closely as possible, but also to denote differences in process between samples.

Most challenges in this research, however, lay not only in the coating application but in understanding the chemical background behind several of the samples. As commercial products were explored for more than half of the hydrophobic coatings to be tested, their parent companies were reluctant to provide proprietary information related to their products, preventing a full depth of background research. Although Kraton has released technical data sheets on all their products for customer use, these offer only enough information for knowledgeable customers to safely use their products in conjunction with other compounds or solutions. The Instron tensile tests suggested that there was also a chemical reaction occurring between the PBO and the Flex Seal coating used, but what this reaction might be is unknown.

To mitigate some of these concerns, all disparities in methods, measurements, and data for this research were noted.

### **C. FUTURE RESEARCH**

This research supports the need for collecting more data in a more in-depth  $V_{50}$  assessment, to better identify and cull outlying penetration velocity data points. The skew towards a faster  $V_{50}$  velocity for the uncoated exposed PBO falls outside of normal variation and places it at a faster  $V_{50}$  velocity than the uncoated unexposed PBO, which does not track with the expected weakening effect of moisture on PBO fiber.

Further refined coating methods should also be explored, to better control the thickness of the waterproof coating on Zylon weave. Proper application equipment may also ensure consistency between industrial-grade Kraton polymer coatings, making them viable alternatives to the Flex Seal liquid coating used in this research.

THIS PAGE INTENTIONALLY LEFT BLANK

## APPENDIX A

Shot	Material	Coated?	Exposed?	Load Cell Offset (lbs)		Gun Pressure (psi)	$\Delta t$ (s)	Velocity (ft/s)	Penetration
				Vertical	Horizontal				
<b>1</b>	UHMWPE Test Shot			2	4	1523	0.000756	1598.28	-
<b>2</b>	UHMWPE Test Shot			2	4	1560	0.000736	1641.71	-
<b>3</b>	UHMWPE Test Shot			2	4	1340	0.000736	1641.71	-
<b>4</b>	PBO	No	No	2	4	850	0.000788	1533.38	Complete
<b>5</b>	PBO	No	No	2	4	530	0.000924	1307.68	Complete
<b>6</b>	PBO	Yes	No	2	4	620	0.001350	895.04	Complete
<b>7</b>	PBO	No	No	2	4	710	0.001120	1078.84	Complete
<b>8</b>	PBO	No	No	2	4	720	0.001010	1196.34	Complete
<b>9</b>	PBO	No	No	2	4	820	0.001020	1184.61	Complete
<b>10</b>	PBO	No	No	2	4	805	0.001010	1196.34	Complete
<b>11</b>	PBO	No	No	2.5	4.5	760	0.000952	1269.22	Complete
<b>12</b>	PBO	No	No	2.5	4.5	728	0.000956	1263.91	Complete
<b>13</b>	PBO	No	No	2.5	4.5	725	0.001010	1196.34	Complete
<b>14</b>	PBO	No	No	3	4.5	700	0.001010	1196.34	Complete
<b>15</b>	PBO	No	No	2.5	5.5	752	0.001020	1184.61	Complete
<b>16</b>	PBO	Yes	No	3.25	6	755	0.000972	1243.11	Complete
<b>17</b>	PBO	Yes	No	3.5	6.5	780	0.000964	1253.42	Complete
<b>18</b>	PBO	Yes	No	2.75	6	850	0.000968	1248.24	Complete
<b>19</b>	PBO	Yes	No	2.75	5.75	850	Data not recorded		Complete
<b>20</b>	PBO	Yes	No	2.5	6	728	0.001000	1208.30	Complete
<b>21</b>	PBO	Yes	No	2.5	5.75	690	0.001020	1184.61	Complete
<b>22</b>	PBO	Yes	No	2.5	6	660	0.001080	1118.80	Complete

Shot	Material	Coated?	Exposed?	Load Cell Offset (lbs)		Gun Pressure (psi)	$\Delta t$ (s)	Velocity (ft/s)	Penetration
				Vertical	Horizontal				
23	PBO	Yes	No	2.75	6	605	0.001130	1069.29	Complete
24	PBO	Yes	No	2.75	6.25	510	0.001080	1118.80	Complete
25	PBO	No	Yes	2.75	6.25	600	0.001560	774.55	Complete
26	PBO	No	Yes	3.5	6	500	0.001740	694.43	Complete
27	PBO	No	Yes	3.5	7	427	0.001100	1098.45	Complete
28	PBO	No	No	4	6.25	620	0.000928	1302.05	Complete
29	PBO	No	No	3.75	6.5	423	0.001220	990.41	Complete
30	PBO	No	No	3.5	6.5	330	0.0011	1098.45	Complete
31	PBO	No	No	3.75	6.25	210	0.00132	915.38	Complete
32	PBO	No	No	4	6.25	160	0.00153	789.74	Complete
33	PBO	No	No	4	6.25	110	0.00172	702.50	Complete
34	PBO	No	No	3.75	6.25	83.5	0.00204	592.30	Complete
35	PBO	No	No	3.75	6.25	57	0.00272	444.23	Partial
36	PBO	No	No	3.75	6.25	69	0.00223	541.84	Complete
37	PBO	No	No	3.75	6.25	62	0.00223	541.84	Complete
38	PBO	No	No	3.75	6.25	57	0.00259	466.53	Partial
39	UHMWPE Test Shot			3.75	6.25	60	0.00236	511.99	-
40	UHMWPE Test Shot			3.75	6.25	68	0.00214	564.63	-
41	UHMWPE Test Shot			3.75	6.25	72	0.00207	583.72	-
42	UHMWPE Test Shot			3.75	6.25	85.5	0.00202	598.17	-
43	PBO	No	No	3.75	6.25	60.5	0.00261	462.95	Complete
44	PBO	Yes	No	3.75	6.5	64	0.00244	495.20	Partial
45	PBO	Yes	No	3.75	6.25	68.5	0.00248	487.22	Partial
46	PBO	Yes	No	3.75	6.25	73.5	0.00218	554.27	Complete
47	PBO	Yes	No	3.75	6.25	71	0.00214	564.63	Complete

Shot	Material	Coated?	Exposed?	Load Cell Offset (lbs)		Gun Pressure (psi)	$\Delta t$ (s)	Velocity (ft/s)	Penetration
				Vertical	Horizontal				
48	PBO	Yes	No	4	6.5	68	0.00234	516.37	Partial
49	PBO	No	Yes	3.75	6.25	56	0.00258	468.33	Complete
50	PBO	No	Yes	3.75	6.25	61	0.00258	468.33	Complete
51	PBO	No	Yes	3.75	6.25	55	0.00297	406.84	Partial
52	PBO	No	Yes	3.75	6.25	58	0.00242	499.30	Uncertain
53	PBO	No	Yes	3.75	6.25	58	0.00236	511.99	Partial
54	PBO	No	Yes	3.75	6.25	62	0.00224	539.42	Partial
55	PBO	No	No	3.75	6.25	52	0.00246	491.18	Partial
56	PBO	Yes	Yes	3.75	6.25	56	0.00237	509.83	Partial
57	PBO	Yes	Yes	3.75	6.25	61	0.00221	546.74	Complete
58	PBO	Yes	Yes	4	5	58	0.00228	529.96	Partial
59	PBO	No	No	3.75	6.25	56	0.00243	497.20	Partial

THIS PAGE INTENTIONALLY LEFT BLANK

## LIST OF REFERENCES

- [1] Toyobo Co., *PBO fiber ZYLON, Technical Information (Revised 2005.6)*, 2005. [Online]. Available: <https://www.toyobo-global.com/seihin/kc/pbo/zylon-p/bussei-p/technical.pdf>
- [2] H. Murase, “History of super fibers: Adventures in quest of the strongest fiber,” in *High-Performance and Specialty Fibers Concepts, Technology and Modern Applications of Man-Made Fibers for the Future*, K. Yabuki, The Society of Fiber Science and Technology, Eds. Tokyo, Japan: Springer Japan, 2016, pp. 83–94.
- [3] D. Tompkins, “Body armor safety initiative,” National Institute of Justice, 2006. Accessed 27 Sep. 2020. [Online]. Available: <https://nij.ojp.gov/topics/articles/body-armor-safety-initiative>.
- [4] S. Bocetta, “The history of body armor: From medieval times to today,” *Small Wars Journal, Small Wars Foundation*, 2017. Accessed 27 Sep. 2020. [Online]. Available: <https://smallwarsjournal.com/jrnl/art/the-history-of-body-armor-from-medieval-times-to-today#:~:text=The%20earliest%20recorded%20types%20of,Wars%2C%20some%20developments%20were%20made>.
- [5] L. King, “Lightweight body armor,” *Lightweight Body Armor, Doron 1953*, 1953. Accessed 27 Sep. 2020. [Online]. Available: [https://qmmuseum.lee.army.mil/korea/lightweight\\_body\\_armor.htm](https://qmmuseum.lee.army.mil/korea/lightweight_body_armor.htm).
- [6] G. A. Holmes, K. Rice, and C. R. Snyder, “Ballistic fibers: A review of the thermal, ultraviolet, and hydrolytic stability of the benzoxazole ring structure,” *Journal of Materials Science*, vol. 41, pp. 4105–4116, 2006.
- [7] H. van der Werff, “High-performance ballistic fibers: Ultra-high molecular weight polyethylene (UHMWPE),” in *Advanced fibrous composite materials for ballistic protection*, X. Chen, Ed. Duxford, Cambridge, UK: Woodland Publishing, 2016, pp. 71–107.
- [8] J. March, *Advanced Organic Chemistry: Reactions, Mechanisms, and Structure*, John Wiley & Sons, New York, pp. 383, 1992.
- [9] K. Bilisik, “Two-dimensional (2D) fabrics and three-dimensional (3D) preforms for ballistic and stabbing protection: A review,” *Textile Research Journal*, vol. 87, no. 18, pp. 2275–2304, 2017.
- [10] “Products,” Kraton Corporation, 2020. Accessed 27 Sep. 2020. [Online]. Available: <https://www.kraton.com/>.

THIS PAGE INTENTIONALLY LEFT BLANK

## **INITIAL DISTRIBUTION LIST**

1. Defense Technical Information Center  
Ft. Belvoir, Virginia
2. Dudley Knox Library  
Naval Postgraduate School  
Monterey, California